

Thermodynamics and Spin Tunneling Dynamics in Ferric Wheels with Excess Spin

Florian Meier and Daniel Loss

Department of Physics and Astronomy, University of Basel, Klingelbergstrasse 82, 4056 Basel, Switzerland
(July 2, 2001)

We study theoretically the thermodynamic properties and spin dynamics of a class of magnetic rings closely related to ferric wheels, antiferromagnetic ring systems, in which one of the Fe (III) ions has been replaced by a dopant ion to create an excess spin. Using a coherent-state spin path integral formalism, we derive an effective action for the system in the presence of a magnetic field. We calculate the functional dependence of the magnetization and tunnel splitting on the magnetic field and show that the parameters of the spin Hamiltonian can be inferred from the magnetization curve. We study the spin dynamics in these systems and show that quantum tunneling of the Néel vector also results in tunneling of the total magnetization. Hence, the spin correlation function shows a signature of Néel vector tunneling, and electron spin resonance (ESR) techniques or AC susceptibility measurements can be used to measure both the tunneling and the decoherence rate. We compare our results with exact diagonalization studies on small ring systems. Our results can be easily generalized to a wide class of nanomagnets, such as ferritin.

75.50.Xx,75.10.Jm,03.65.Sq,73.40.Gk

I. INTRODUCTION

Nanomagnets and molecular clusters are systems in which macroscopic quantum phenomena may be observed in the form of quantum tunneling of the magnetization.¹⁻³ Two scenarios must be carefully distinguished: incoherent macroscopic quantum tunneling (MQT) and macroscopic quantum coherence (MQC). In the latter case, tunneling between energetically degenerate spin configurations takes place at a rate Δ/h large compared to the spin decoherence rate Γ . In ferromagnetic molecular clusters such as Fe_8 and Mn_{12} the ground state tunnel splitting Δ is small compared to $\hbar\Gamma$.⁴⁻⁶ However, Δ is significantly larger in antiferromagnetic (AF) systems^{7,8} which are promising candidates for the observation of MQC in the form of coherent tunneling of the Néel vector \mathbf{n} .

The ferric wheels (FWs) $\text{Li}:\text{Fe}_6$, $\text{Na}:\text{Fe}_6$, $\text{Cs}:\text{Fe}_8$, and Fe_{10} ⁹⁻¹⁴ are a particularly interesting class of molecular magnets. The $s = 5/2$ Fe (III) ions are arranged on a ring, with an AF nearest-neighbor exchange coupling $J > 0$, and a weak, easy-axis anisotropy (k_z) directed along the ring axis \mathbf{e}_z . For $h_x = 0$, the classical ground-state spin configuration has alternating (Néel) order with the spins pointing along $\pm\mathbf{e}_z$. The two states with the Néel vector \mathbf{n} along $\pm\mathbf{e}_z$ [Fig. 1], labeled $|\uparrow\rangle$ and $|\downarrow\rangle$, are energetically degenerate and separated by an energy barrier of height $Nk_z s^2$. However, $|\uparrow\rangle$ and $|\downarrow\rangle$ are not energy eigenstates. Rather, the low-energy sector of the FW consists of a ground state $|g\rangle = (|\uparrow\rangle + |\downarrow\rangle)/\sqrt{2}$ and a first excited state $|e\rangle = (|\uparrow\rangle - |\downarrow\rangle)/\sqrt{2}$, separated in energy by Δ . For weak tunneling, $|g\rangle$ and $|e\rangle$ are energetically well separated from all other energy eigenstates.

For Fe_{10} , the tunnel splitting Δ can be as large as 2.18K.^{14,15} An estimate for the electron spin decoherence rate Γ in FWs can be obtained from the typical

energy scales of the various interactions of the electron spins. These include nuclear dipolar interactions with ^1H nuclei (0.1mK [Ref. 16]), hyperfine interactions with ^{57}Fe (1mK [Ref. 17]), and interring electron spin dipolar interactions (of order 10-50mK), and possible interring superexchange processes, which are difficult to estimate but may be of order 100mK. However, the tunnel splitting is sufficiently large that FWs are most promising candidates for coherent tunneling of \mathbf{n} even in the presence of intrinsic or extrinsic sources of decoherence on energy scales up to 0.5K.

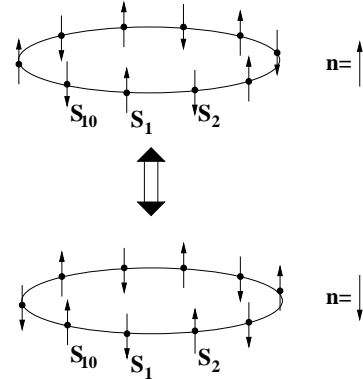


FIG. 1. The two degenerate classical ground-state spin configurations of the ferric wheel Fe_{10} .

Although quantum tunneling effects in antiferromagnets are more pronounced than in ferromagnets,^{7,8} the detection of quantum behavior is experimentally more challenging. The reason for this is that magnetization and susceptibility measurements probe only the total spin of the molecule which, by symmetry, remains unaltered upon tunneling of the Néel vector. This problem is resolved in ferrimagnets and antiferromagnets with uncompensated sublattice spins, in which Δ is still large and

tunneling of \mathbf{n} leads to large signals in the alternating-current (AC) susceptibility,^{18–20} provided that magnetic fields are small.^{21–24} Recent work²⁵ indicates that ferrimagnets exhibit a wealth of interesting tunnel scenarios also in finite magnetic fields.

In this paper we study magnetic rings closely related to the ferric wheels, in which one of the Fe (III) ions has been replaced by a Ga or Cr ion with spin $s' = 0$ or $s' = 3/2$, respectively, to create an excess spin. Such systems have been synthesized recently.²⁶ Starting from a microscopic model Hamiltonian,

$$\hat{H} = J \sum_{i=2}^{N-1} \hat{\mathbf{s}}_i \cdot \hat{\mathbf{s}}_{i+1} + J'(\hat{\mathbf{s}}_1 \cdot \hat{\mathbf{s}}_2 + \hat{\mathbf{s}}_1 \cdot \hat{\mathbf{s}}_N) + \hbar \mathbf{h} \cdot \sum_{i=1}^N \hat{\mathbf{s}}_i - (k'_z \hat{s}_{1,z}^2 + k_z \sum_{i=2}^N \hat{s}_{i,z}^2), \quad (1)$$

which also accounts for modified exchange (J') and anisotropy (k'_z) constants due to doping, we calculate various thermodynamic quantities and spin correlation functions. In Eq. (1), $N = 10, 8$, or 6 , $\mathbf{h} = g\mu_B \mathbf{B}/\hbar$, with \mathbf{B} the external magnetic field, and $g = 2$ is the electron spin g -factor. As we will show, the excess spin $\delta s = s' - s$ is strongly coupled to \mathbf{n} and hence is expected to modify both the thermodynamic properties and the spin dynamics of the FW. In contrast, for an impurity spin coupled weakly to the Néel vector,²⁷ the thermodynamic properties of the wheel remain essentially unaltered. For the modified FWs discussed in the present work, Néel vector tunneling also leads to oscillations of the total spin which are in principle observable in AC susceptibility or ESR measurements. Thermodynamic properties of AF systems with uncompensated sublattice spins by now have been studied in great detail for various anisotropy potentials and field configurations.^{28,29} One main advantage of the small, high-symmetry modified FW studied in the present work is that the dependence of various thermodynamic quantities and spin correlation functions on the small number of microscopic parameters entering Eq. (1) can be evaluated analytically.

The outline of this paper is as follows. In Sec. II we review the theory of spin tunneling in FWs and calculate the spin correlation functions $\chi_{\alpha\alpha}$. In Sec. III we discuss the modified FW within a classical vector model and show that, in contrast to the FW, tunneling of \mathbf{n} now also results in oscillations of the total spin. In Sec. IV and Sec. V, we develop a semiclassical theory of the modified FW, thus generalizing earlier work on AF systems with uncompensated sublattice spins^{21–24} to $B_x \neq 0$. For $|J'/J - 1| \ll 1$, we evaluate explicitly the tunnel splitting $\tilde{\Delta}$ and magnetization M_x of the modified FW, and show that J' can be determined by measuring M_x . We calculate the Fourier transform of the real-time susceptibility $\chi''_{zz}(\omega \simeq \tilde{\Delta}/\hbar)$ and prove that Néel vector tunneling can be detected in AC susceptibility or ESR measurements. In Sec. VI, we discuss the modified FW for the limiting

cases $J'/J \gg 1$ and $J'/J \ll 1$. The relevance of the present work for experiments is discussed in Sec. VII. Finally, we indicate that our results can be easily generalized to other systems such as ferritin (Sec. VIII). We summarize our results in Sec. IX.

II. THERMODYNAMICS AND SPIN DYNAMICS OF THE FW

A. Thermodynamics

In this section, we give a brief review of previous work on Néel vector tunneling in FWs.¹⁴ In particular, we point out that the notion of quantum tunneling applies only to Fe₁₀ and Cs:Fe₈ (and somewhat less to Na:Fe₆) for large h_x , but not to Li:Fe₆.

The minimal Hamiltonian of the FWs contains only two parameters, J and k_z ,

$$\hat{H}_0 = J \sum_{i=1}^N \hat{\mathbf{s}}_i \cdot \hat{\mathbf{s}}_{i+1} + \hbar \mathbf{h} \cdot \sum_{i=1}^N \hat{\mathbf{s}}_i - k_z \sum_{i=1}^N \hat{s}_{i,z}^2. \quad (2)$$

Here $N = 10, 8$, or 6 and $\hat{\mathbf{s}}_{N+1} \equiv \hat{\mathbf{s}}_1$, $\mathbf{h} = g\mu_B \mathbf{B}/\hbar$, with \mathbf{B} the external magnetic field, and $g = 2$ is the electron spin g -factor. Throughout this paper we restrict our attention to $\mathbf{B} = B_x \mathbf{e}_x$, i.e. magnetic fields applied in the ring plane. For $k_z = 0$, the eigenstates of the total spin $\hat{\mathbf{S}} = \sum_{i=1}^N \hat{\mathbf{s}}_i$ are also energy eigenstates, with energy^{10,14} $E_{S,S_x} \simeq (2J/N)S(S+1) + \hbar h_x S_x$. For systems with weak anisotropy, $k_z \ll 2J/(Ns)^2$, the anisotropy can be taken into account in perturbation theory for a wide range of h_x . However, the scenario changes for large anisotropy $k_z \gtrsim 2J/(Ns)^2$, where mixing of different spin multiplets becomes appreciable, as is the case for Fe₁₀, Cs:Fe₈, and Na:Fe₆.

Both the tunnel splitting Δ and the magnetization M_x of the FW can be obtained from the partition function $Z_0[h_x]$ which we evaluate using spin path integrals. Introducing spin coherent states, we decompose the local spin fields \mathbf{s}_i ³⁰

$$\mathbf{s}_i = (-1)^{i+1} s \mathbf{n} + \mathbf{l} \quad (3)$$

into a Néel ordered field $\pm s \mathbf{n}$ ($\mathbf{n}^2 = 1$) and fluctuations $\mathbf{l} \perp \mathbf{n}$ around it. For small systems containing 6, 8, or 10 spins, spatial fluctuations of the fields \mathbf{n} and \mathbf{l} are frozen out at low temperature T . Carrying out the Gaussian integral over \mathbf{l} , we obtain $Z_0 = \int \mathcal{D}\mathbf{n} \exp \left[- \int_0^{\beta\hbar} d\tau L_0[\mathbf{n}]/\hbar \right]$ with a Euclidean Lagrangean depending only on \mathbf{n} ,

$$L_0[\mathbf{n}] = \frac{N\hbar^2}{8J} [-(i\mathbf{n} \times \dot{\mathbf{n}} - \mathbf{h})^2 + (\mathbf{h} \cdot \mathbf{n})^2 - \omega_0^2 n_z^2], \quad (4)$$

where $\omega_0 = s\sqrt{8Jk_z}/\hbar$.

In contrast to the classical description of the states $|\uparrow\rangle$ and $|\downarrow\rangle$ used in Sec. I, in a quantum mechanical treatment \mathbf{n} always exhibits quantum fluctuations around its classical minima. The notion of quantum tunneling, however, is only applicable if \mathbf{n} is well localized in the states $|\uparrow\rangle$ and $|\downarrow\rangle$, i.e. if $1 - \langle n_z^2 | \uparrow \rangle \ll 1$. The quantum fluctuations of \mathbf{n} can be estimated from Eq. (4). For $\mathbf{h} = 0$, L_0 describes two independent harmonic oscillators of frequency ω_0 , corresponding to fluctuations of \mathbf{n} in the direction of \mathbf{e}_x and \mathbf{e}_y . If the amplitude of the fluctuations is small, we can evaluate the mean deviation of the Néel vector from \mathbf{e}_z , $1 - \langle n_z^2 \rangle \simeq 2/(\mathcal{S}_0/\hbar)$, where $\mathcal{S}_0/\hbar = Ns\sqrt{2k_z/J}$ is the classical tunnel action. Hence, \mathbf{n} is well localized along \mathbf{e}_z only if $\mathcal{S}_0/\hbar \gg 2$ or, equivalently, if the ground-state energy, $2 \times \omega_0/2$, is small compared to the potential barrier $Nk_z s^2$. The scenario changes if a strong magnetic field $\mathbf{h} = h_x \mathbf{e}_x$, $h_x \gg \omega_0$, is applied in the ring plane. Then, the mode of \mathbf{n} along \mathbf{e}_x is frozen out, such that $1 - \langle n_z^2 \rangle \simeq 1/(\mathcal{S}_0/\hbar)$, and the FW can exhibit quantum tunneling if $\mathcal{S}_0/\hbar \gg 1$. Note that for large tunnel action, $\mathcal{S}_0/\hbar \gtrsim 10$, the tunnel splitting becomes small, which would make the system under consideration a less favorable candidate for the observation of MQC.

The FWs Li:Fe₆, Na:Fe₆, Cs:Fe₈, and Fe₁₀ have been well characterized.^{10–13,15,31} For Fe₁₀, $J = 15.56\text{K}$ and $k_z = 0.0088J$. For Cs:Fe₈, $J = 22.5\text{K}$ and $k_z = 0.0191J$.¹³ For Fe₆, J and k_z vary appreciably depending on the central alkali metal ion and ligands: for Na:Fe₆, $J = 32.77\text{K}$ and $k_z = 0.0136J$, whereas for Li:Fe₆, $J = 20.83\text{K}$ and $k_z = 0.0053J$.^{31,15} In Table I, \mathcal{S}_0/\hbar and $\hbar\omega_0/2\mu_B$ are given for Fe₁₀, Cs:Fe₈, Na:Fe₆, and Li:Fe₆. As is obvious from these values, for none of the molecular rings \mathcal{S}_0/\hbar is sufficiently large to assure that a tunnel scenario is rigorously applicable if $h_x \lesssim \omega_0$. In Na:Fe₆, even at large $B_x \gg 20\text{T}$, \mathbf{n} is far less well localized along \mathbf{e}_z than in Fe₁₀, which hence remains the most favorable candidate for the observation of quantum tunneling. Note however that even in Fe₁₀ and Cs:Fe₈, \mathcal{S}_0/\hbar is so small that corrections to the instanton techniques used below may become large.³²

	\mathcal{S}_0/\hbar	$\hbar\omega_0/2\mu_B$
Fe ₁₀	3.32	7.68 T
Cs:Fe ₈	3.91	16.37T
Na:Fe ₆	2.47	20.11T
Li:Fe ₆	1.54	7.98T

TABLE I. $\mathcal{S}_0/\hbar = Ns\sqrt{2k_z/J}$ and $\hbar\omega_0/2\mu_B$ for Fe₁₀, Cs:Fe₈, Na:Fe₆, and Li:Fe₆.

For $h_x \gg \omega_0$, the magnetic field \mathbf{B} strongly confines \mathbf{n} to the (y, z) -plane and thus determines the tunnel path of the electron spins. This allows one to evaluate Z_0 . We parameterize

$$\mathbf{n} = (\cos \theta, \sin \theta \cos \phi, \sin \theta \sin \phi) \quad (5)$$

and expand L_0 to second order in $\vartheta = \theta - \pi/2$,

$$L_0[\mathbf{n}] = \frac{N\hbar^2}{8J} [-(h_x - i\dot{\phi})^2 - \omega_0^2 \sin^2 \phi] + \frac{1}{2} \vartheta G^{-1}[\phi] \vartheta, \quad (6)$$

where $G^{-1}[\phi] = (N\hbar^2/4J)(-\partial_\tau^2 + (h_x - i\dot{\phi})^2 + \omega_0^2 \sin^2 \phi)$, $\dot{\phi} = \partial_\tau \phi$, and $\omega_0 = s\sqrt{8Jk_z}/\hbar$ as defined above. The typical energy scales for the dynamics of ϕ and ϑ are ω_0 and h_x , respectively. Due to this separation of energy-scales, we can use an adiabatic approximation, in which ϑ oscillates rapidly in a quasistatic harmonic potential³³ $(N\hbar^2/8J)(h_x^2 - 2ih_x\dot{\phi})$. Integrating out ϑ , we obtain an expression for L_0 depending only on ϕ .¹⁴ For $k_B T/\hbar \ll \omega_0 \ll h_x$, we find

$$L_0[\phi] \simeq \frac{N\hbar^2}{8J} [-(h_x - i\dot{\phi})^2 - \omega_0^2 \sin^2 \phi] + \hbar \frac{h_x - i\dot{\phi}}{2} + \mathcal{O}(\omega_0^2/h_x), \quad (7)$$

where the term $\hbar(h_x - i\dot{\phi})/2$ arises from the ϑ fluctuation determinant. The two saddle-points of Eq. (7), $\phi \equiv \pi/2$ and $\phi \equiv 3\pi/2$, correspond to the two classical spin configurations sketched in Fig. 1. If tunneling is weak, $\mathcal{S}_0/\hbar \gg 1$, the remaining path integral over ϕ is straightforward.^{34,14} Summing all multi-instanton solutions, one finds

$$Z_0 = \exp \left[\beta \left(\frac{N\hbar^2}{8J} h_x^2 - \hbar \frac{h_x + \omega_0}{2} \right) \right] \cosh \left(\frac{\beta \Delta(h_x)}{2} \right) \quad (8)$$

with the tunnel splitting

$$\Delta(h_x) = \Delta_0 \left| \sin \left(\pi \frac{N\hbar}{4J} h_x \right) \right|, \quad (9)$$

where $\beta = 1/k_B T$, $\Delta_0 = 8\hbar\omega_0 \sqrt{\mathcal{S}_0/2\pi\hbar} \exp[-\mathcal{S}_0/\hbar]$, and $\mathcal{S}_0/\hbar = Ns\sqrt{2k_z/J}$. In particular, Δ is periodic as a function of h_x . Differentiating with respect to B_x , we obtain the magnetization¹⁴

$$M_x = (g\mu_B) \left[\frac{N\hbar}{4J} h_x - \frac{1}{2} + \frac{1}{2\hbar} \frac{\partial \Delta}{\partial h_x} \tanh \left(\frac{\beta \Delta}{2} \right) \right]. \quad (10)$$

Because $\partial \Delta / \partial h_x$ is discontinuous at the zeroes of Δ , M_x exhibits steps at $B_{c,n} = n4J/Ng\mu_B$, where $n = 1, 2, \dots, Ns$. From

$$M_\alpha = (g\mu_B) \frac{N\hbar}{4J} \frac{1}{Z} \int \mathcal{D}\mathbf{n} [h_\alpha - i(\mathbf{n} \times \dot{\mathbf{n}})_\alpha - n_\alpha \mathbf{h} \cdot \mathbf{n}] \times e^{-\int_0^{\beta\hbar} d\tau L_0[\mathbf{n}]/\hbar}, \quad (11)$$

it also follows that, for arbitrary h_x , $M_\alpha = 0$ for $h_\alpha = 0$, $\alpha = y, z$, which is a result of the invariance of \hat{H}_0 under rotation around \mathbf{B} by π .³⁵

B. Spin dynamics

We show now that the tunneling dynamics of \mathbf{n} does not enter the susceptibility of the FW, i.e. that the imaginary part of the susceptibility, $\chi''_{\alpha\alpha}(\omega)$, has no absorption peak $\delta(\omega - \Delta/\hbar)$. To prove this, we calculate the susceptibility of the total spin, $\hat{\mathbf{S}} = \sum_{i=1}^N \hat{\mathbf{s}}_i$, in Matsubara representation,

$$\chi_{\alpha\alpha}(i\omega_n) = (g\mu_B)^2 \int_0^{\beta\hbar} d\tau e^{i\omega_n\tau} [\langle T_\tau \hat{S}_\alpha(\tau) \hat{S}_\alpha(0) - \langle \hat{S}_\alpha \rangle^2 \rangle], \quad (12)$$

where $\alpha = x, y, z$. As we will show below, $\chi_{\alpha\alpha}(i\omega_n)$ contains *no* terms proportional to $1/(i\omega_n - \Delta/\hbar)$. This implies that AC susceptibility or ESR measurements cannot be used to detect Néel vector tunneling in FWs described by \hat{H}_0 .

$\chi_{xx}(i\omega_n)$ can be calculated from the generating functional $Z[\delta h_x(\tau)]$, where $\delta h_x(\tau)$ is a small probing field added to the static field $h_x \gg \omega_0$. Because we are only interested in the low frequency response of the FW, $\omega_n \lesssim \Delta/\hbar \ll \omega_0$, we may restrict our attention to a slowly varying field δh_x whose Fourier components vanish for $\omega_n \gtrsim \Delta/\hbar$. The typical timescale for dynamics of ϕ , $1/\omega_0$, is short compared to the timescale on which δh_x varies. In particular, approximating $\delta h_x(\tau)$ by a constant during instanton passage, we find

$$Z[\delta h_x(\tau)] \simeq \exp\left[\int_0^{\beta\hbar} \frac{d\tau}{\hbar} \left(\frac{N\hbar^2}{8J} (h_x + \delta h_x(\tau))^2 - \hbar \frac{h_x + \delta h_x(\tau) + \omega_0}{2} \right)\right] \cosh\left[\int_0^{\beta\hbar} \frac{d\tau}{\hbar} \frac{\Delta(h_x + \delta h_x(\tau))}{2}\right]. \quad (13)$$

Differentiating twice and setting $\delta h_x \rightarrow 0$, for $\omega_n \lesssim \Delta/\hbar$,

$$\chi_{xx}(i\omega_n) = (g\mu_B)^2 \left[\frac{N\hbar}{4J} + \frac{1}{2\hbar} \frac{\partial^2 \Delta}{\partial h_x^2} \tanh(\beta\Delta/2) + \frac{\beta}{\hbar} \left(\frac{1}{2} \frac{\partial \Delta}{\partial h_x} \right)^2 \cosh^{-2}(\beta\Delta/2) \delta_{\omega_n,0} \right]. \quad (14)$$

The transverse susceptibilities can be evaluated directly from $\delta^2 Z / \delta h_\alpha(\tau) \delta h_\alpha(0)$, $\alpha = y, z$. Using the parametrization in Eq. (5), $\vartheta = \theta - \pi/2$ can be integrated out in the path-integral expression for $\chi_{\alpha\alpha}$. After lengthy calculation (Appendix A), we obtain for $\omega_n \ll h_x$

$$\begin{aligned} \chi_{yy}(i\omega_n) &\simeq (g\mu_B)^2 \frac{N\hbar}{4J}, \\ \chi_{zz}(i\omega_n) &\simeq (g\mu_B)^2 \frac{N\hbar}{4J}. \end{aligned} \quad (15)$$

From Eqs. (14) and (15) it is evident that none of the susceptibilities $\chi_{\alpha\alpha}(i\omega_n)$ contains a term proportional to $1/(i\omega_n \pm \Delta/\hbar)$. In the tunneling regime discussed here, $|g\rangle$ and $|e\rangle$ are energetically well separated from all other states. Then, Eq. (15) and the spectral representation

$$\chi_{\alpha\alpha}(i\omega_n) = \sum_{i,j} \frac{e^{-\beta E_i}}{Z} |\langle i | \hat{S}_\alpha | j \rangle|^2 \left(\frac{1}{i\omega_n - (E_i - E_j)/\hbar} - \frac{1}{i\omega_n + (E_i - E_j)/\hbar} \right) - \beta \hbar \delta_{\omega_n,0} \langle \hat{S}_\alpha \rangle^2 \quad (16)$$

where $|i\rangle$ and $|j\rangle$ label energy eigenstates, imply that $\langle e | \hat{S}_\alpha | g \rangle = 0$ ($\alpha = x, y, z$). Although for the parameters of Fe₁₀, Cs:Fe₈, and Na:Fe₆ tunnel corrections to $\chi_{\alpha\alpha}$ neglected in Eq. (15) can be significant, the main conclusion of our calculation – that coherent tunneling of \mathbf{n} does not enter the susceptibilities $\chi_{\alpha\alpha}$ – remains valid.

Indeed, $\langle e | \hat{S}_\alpha | g \rangle = 0$ is a direct consequence of the invariance of \hat{H}_0 as $i \rightarrow i+1$, i.e. the exchange of the two sublattices of the bipartite AF ring. In order to clarify this point, we introduce the sublattice spin operators

$$\hat{\mathbf{S}}_A = \sum_{i=\text{odd}} \hat{\mathbf{s}}_i, \quad \hat{\mathbf{S}}_B = \sum_{i=\text{even}} \hat{\mathbf{s}}_i. \quad (17)$$

with $\hat{\mathbf{S}} = \hat{\mathbf{S}}_A + \hat{\mathbf{S}}_B$. In a semiclassical description of the FW, spins of one sublattice couple ferromagnetically to each other. The classical spin fields³⁰ \mathbf{s}_i then obey $\mathbf{s}_i = \mathbf{S}_A/(N/2)$ for odd i , and $\mathbf{s}_i = \mathbf{S}_B/(N/2)$ for even i . This amounts to treating \mathbf{S}_A and \mathbf{S}_B as single large spins^{7,8,22} with spin quantum number $Ns/2$, and \hat{H}_0 reduces to

$$\begin{aligned} \hat{H}_{0,\text{subl}} &= \frac{4J}{N} \hat{\mathbf{S}}_A \cdot \hat{\mathbf{S}}_B + \hbar \mathbf{h} \cdot (\hat{\mathbf{S}}_A + \hat{\mathbf{S}}_B) \\ &\quad - \frac{2k_z}{N} (\hat{S}_{A,z}^2 + \hat{S}_{B,z}^2). \end{aligned} \quad (18)$$

Similar to the nonlinear sigma model (NLSM)-formalism used above, $\hat{H}_{0,\text{subl}}$ provides an appropriate description of the low-energy physics of the FW.

In Fig. 2, the two classical ground-state spin configurations of $\hat{H}_{0,\text{subl}}$ are shown. A finite magnetic field \mathbf{B} tilts the sublattice spins away from the direction of \mathbf{B} such that $\mathbf{S} = \mathbf{S}_A + \mathbf{S}_B$ is parallel to \mathbf{B} . During tunneling of \mathbf{n} , the sublattice spins retain their position relative to each other and rotate jointly around \mathbf{e}_x . The total spin vector \mathbf{S} , however, remains invariant during tunneling such that the real-time spin correlation function does not contain terms proportional to $e^{i\Delta t/\hbar}$ or, equivalently, $\langle e | \hat{S}_\alpha | g \rangle = 0$.

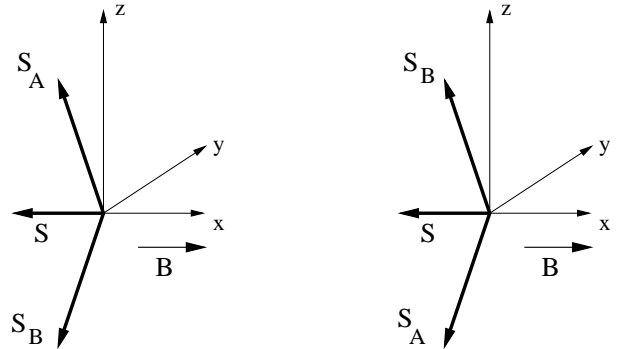


FIG. 2. Sublattice spins and total spin of the FW in magnetic fields.

III. A PHENOMENOLOGICAL MODEL FOR THE MODIFIED FW

The fact that the susceptibilities $\chi_{\alpha\alpha}$ of the FW show no signature of the tunneling of \mathbf{n} is a consequence of the symmetry of $\hat{H}_{0,\text{subl}}$ under $\hat{\mathbf{S}}_A \leftrightarrow \hat{\mathbf{S}}_B$. In the modified FWs [Eq. (1)] this symmetry is broken, which makes them much more suitable for the observation of tunneling of \mathbf{n} . In this section we discuss the saddle-point, i.e. classical, properties of the phenomenological sublattice model for the modified FW. We generalize earlier work²¹⁻²⁴ to finite magnetic fields and show that, in contrast to systems with easy-plane anisotropy,²⁵ in molecular rings with easy-axis anisotropy and finite excess spin, \mathbf{S} oscillates as \mathbf{n} tunnels.

Following Sec. II B, we introduce $\hat{\mathbf{S}}_A$ and $\hat{\mathbf{S}}_B$ as defined in Eq. (17). The Hamiltonian \hat{H} of the modified FW can thus be mapped onto a simpler version in terms of sublattice spins,

$$\hat{H}_{\text{subl}} = \frac{4[(N-2)Js^2 + 2J's's']}{(Ns + 2\delta s)Ns} \hat{\mathbf{S}}_A \cdot \hat{\mathbf{S}}_B + \hbar\mathbf{h} \cdot (\hat{\mathbf{S}}_A + \hat{\mathbf{S}}_B) - \frac{2k_z}{N} \left[\frac{1 + 2(k'_z s'^2 - k_z s^2)/(Nk_z s^2)}{(1 + 2\delta s/Ns)^2} \hat{S}_{A,z}^2 + \hat{S}_{B,z}^2 \right], \quad (19)$$

where $\delta s = s' - s$, $S_A = (N/2 - 1)s + s' = Ns/2 + \delta s$, and $S_B = Ns/2$. Throughout this paper we assume the following inequalities:

$$|\delta s| \ll Ns, \quad (20)$$

$$|k'_z s'^2 - k_z s^2| \ll Nk_z s^2/2, Js, \quad (21)$$

$$2J's' \ll NJs, \quad (22)$$

where $J, J' > 0$. Eq. (20) guarantees that the modified FW is an AF system with small excess spin, to which the theory of Néel vector tunneling applies. Both for Cr and Ga dopant ions ($|\delta s| = 1$ and $5/2$, respectively), Eq. (20) is well satisfied. Eq. (21) will allow us to treat the difference in sublattice anisotropies, $(k'_z s'^2 - k_z s^2)$, in perturbation theory. Typical values of k'_z and k_z are on the order of only $0.01J$, such that this condition holds for most systems of interest. Finally, Eq. (22) together with Eq. (20) assures that the ‘bulk’ parameters of a FW are only slightly altered by exchanging one single spin, such that the parameters of the undoped FW [Table I] still determine whether the modified FW is in a quantum tunneling regime. However, as will be shown below, the excess spin $\delta s \neq 0$ leads to qualitative changes in both thermodynamic and dynamic quantities. We further assume

$$k_B T \ll \hbar\omega_0, \quad (23)$$

which allows us to restrict our attention to the low-energy sector of the FW, which consists of two tunnel-split states only.

We first discuss the classical vector model of Eq. (19) for $k_z = k'_z = 0$, but finite h_x . For an AF system with

equal sublattice spins, the spins would lie close to the plane perpendicular to the field h_x . As sketched in Fig. 2, tilting of the spins leads to a gain in energy $N\hbar^2 h_x^2/8J$. However, for uncompensated sublattices, the configuration sketched in Fig. 3a provides an energy gain $|\delta s|\hbar h_x$ and hence is favorable for $\hbar h_x \ll |\delta s|8J/N = \hbar h_c$. Only for $h_x \gg h_c$, the classical ground-state spin configuration is as sketched in Fig. 3b. The energy is minimized if the projections of \mathbf{S}_A and \mathbf{S}_B onto the (y, z) -plane are antiparallel, such that $\mathbf{S} = \mathbf{S}_A + \mathbf{S}_B$ is parallel to \mathbf{B} . This picture remains valid for a system with easy-plane anisotropy and \mathbf{B} applied in the easy plane.²⁵

The scenario changes for easy-axis (\mathbf{e}_z) anisotropy and a magnetic field \mathbf{B} perpendicular to \mathbf{e}_z . First, the anisotropy favors the spin configuration sketched in Fig. 3b over that in Fig. 3a. The true classical ground-state spin configuration depends on the ratio $k_z/\hbar h_x$. More important, even for $h_x \gg h_c$, \mathbf{S} now has a component perpendicular to \mathbf{B} . The reason for this is that for $\delta s \neq 0$ or $k'_z s'^2 - k_z s^2 \neq 0$, Eq. (19) is no longer invariant under exchange of \mathbf{S}_A and \mathbf{S}_B if $k_z \neq 0$. Due to Eq. (21) and (22), the components S_y and S_z of the total spin can be evaluated perturbatively. With the polar angle ϕ parameterizing the projection of \mathbf{S}_A onto the (y, z) -plane, to leading order in δs and $(k'_z s'^2 - k_z s^2)/2Js$ we obtain

$$\begin{pmatrix} S_y \\ S_z \end{pmatrix} \simeq \left(\delta s \frac{\omega_0^2}{h_x^2} + \frac{k'_z s'^2 - k_z s^2}{2Js} \right) \sin^2 \phi \begin{pmatrix} \cos \phi \\ \sin \phi \end{pmatrix}. \quad (24)$$

As is evident from Eq. (24), finite S_y or S_z can be due to $\delta s \neq 0$ or $k'_z s'^2 - k_z s^2 \neq 0$, i.e. excess spin or unequal effective anisotropies for \mathbf{S}_A and \mathbf{S}_B .

According to Eq. (20), the modified FW is an AF system with small excess spin which is expected to exhibit spin tunnel dynamics qualitatively similar to the FW, as indicated by the close formal analogy between Eqs. (18) and (19). For magnetic fields

$$\max[\hbar\omega_0, |\delta s|8J/N] \ll \hbar h_x \ll 4Js, \quad (25)$$

the sublattice spin vectors \mathbf{S}_A and \mathbf{S}_B lie close to the (y, z) -plane. Due to the easy-axis anisotropy, configurations with \mathbf{S}_A and \mathbf{S}_B close to the z -axis are energetically favorable. It is noteworthy that the condition $h_x \gg \omega_0$ is not indispensable for quantum tunneling of \mathbf{n} , but only assures that a tunnel scenario remains applicable for a wider range of k_z [Sec. II A]. In contrast, $\hbar h_x \gg |\delta s|8J/N$ guarantees that there are two energetically degenerate, macroscopically distinct spin configurations between which spin tunneling may take place²⁵ and hence, in general, will shift the range of magnetic fields in which a tunneling scenario as discussed in the present context [Fig. 1] is valid. Henceforth, we will always assume that B_x is large enough to satisfy Eq. (25). For sufficiently large k_z , the two-state model for the low energy sector of the system outlined in Sec. I then still

applies. As Eq. (24) indicates, the modified FW exhibits one important novel feature: as \mathbf{n} tunnels between \mathbf{e}_z and $-\mathbf{e}_z$ ($\phi = \pi/2$ and $\phi = 3\pi/2$, respectively), the z -component of the total spin, S_z , oscillates between $S_0 = (\delta s \omega_0^2/h_x^2 + (k'_z s'^2 - k_z s^2)/2Js)$ and $-S_0$.

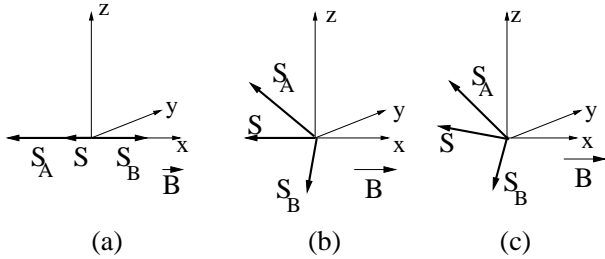


FIG. 3. Classical ground-state spin configurations (schematically) of an AF system with excess spin in a magnetic field. (a) $k_z = k'_z = 0$ and $h_x < h_c = |\delta s|8J/N\hbar$. (b) $h_x > h_c$ and $k_z = k'_z = 0$. (c) $h_x > h_c$. Now, the finite anisotropies $k_z, k'_z \neq 0$ lead to a finite component S_z perpendicular to the magnetic field \mathbf{B} .

IV. THERMODYNAMICS OF THE MODIFIED FW

In order to quantify the statements on Néel vector tunneling in modified FWs [Sec. III], we now develop a semiclassical theory of the modified FW. In this section, we discuss thermodynamic quantities such as the magnetization M_x and specific heat c_v . While our theory treats the spins semiclassically, we give the explicit dependence on the microscopic parameters of \hat{H} [Eq. (1)]. To this end we evaluate the partition function Z , thus generalizing the procedure reviewed in Sec. II A to systems with $k'_z \neq k_z$, $J' \neq J$, and $\delta s \neq 0$. The most significant change is that, for $\delta s \neq 0$, the staggering [Eq. (3)] must be modified in order to account for $\mathbf{s}_1^2 = s'^2$. The ansatz

$$\begin{aligned} \mathbf{s}_1 &= s' \mathbf{n} + \frac{s'}{s} \mathbf{l}, \\ \mathbf{s}_i &= (-1)^{i+1} s \mathbf{n} + \mathbf{l} \quad \forall i \neq 1 \end{aligned} \quad (26)$$

is equivalent to the assumption that spins within sublattices A and B are ferromagnetically coupled.^{7,8,21–24} The results for the magnetization M_x and susceptibilities obtained from this ansatz turn out to be in good agreement with those obtained from numerical exact diagonalization (ED) (see below and Sec. V) as long as $|J'/J - 1| \ll 1$. We restrict ourselves to this case first and discuss further limiting cases $J' \ll J$ and $J' \gg J$ in Sec. VI.

As for the FW,¹⁴ at low temperatures spatial variations of the Néel field \mathbf{n} , and the fluctuations \mathbf{l} around it, are suppressed in small ring system. With the coherent spin states defined in Eq. (26),³⁶

$$Z = \int \mathcal{D}\mathbf{n} \mathcal{D}\mathbf{l} \delta(\mathbf{n} \cdot \mathbf{l}) e^{-S[\mathbf{n}, \mathbf{l}]/\hbar}, \quad (27)$$

where

$$\begin{aligned} S[\mathbf{n}, \mathbf{l}] &= -i\hbar \left(s' \omega[\mathbf{n} + \frac{1}{s} \mathbf{l}] + s \sum_{i=2}^N \omega[(-1)^{i+1} \mathbf{n} + \frac{1}{s} \mathbf{l}] \right) \\ &\quad + \int_0^{\beta\hbar} d\tau H[\mathbf{n}, \mathbf{l}]. \end{aligned} \quad (28)$$

Here,

$$\begin{aligned} H[\mathbf{n}, \mathbf{l}] &= 2[(N-2)J + 2\frac{s'}{s}J']\mathbf{l}^2 + \hbar(N + \frac{\delta s}{s})\mathbf{h} \cdot \mathbf{l} \\ &\quad - [(N-1)k_z s^2 + k'_z s'^2]n_z^2 + \frac{2}{s}(k_z s^2 - k'_z s'^2)n_z l_z \\ &\quad + \delta s \hbar \mathbf{h} \cdot \mathbf{n} \end{aligned} \quad (29)$$

is the classical energy of a given spin configuration. The small term $[(N-1)k_z + k'_z]l_z^2$ has already been neglected. The first term in Eq. (28) is the Berry-phase term, where $\omega[\Omega]$ denotes the area traced out by some vector $\Omega(\tau)$ on the unit sphere. Here, we use the south pole gauge (i.e. $\omega[\Omega(\tau) \equiv -\mathbf{e}_x] = 0$). Expanding the Berry-phase term to leading order in \mathbf{l} with the parametrization Eq. (5) yields

$$- \int_0^{\beta\hbar} d\tau \left[i\delta s \dot{\phi}(1 + \cos\theta) + i(N + \frac{\delta s}{s})(\mathbf{n} \times \dot{\mathbf{n}}) \cdot \mathbf{l} \right]. \quad (30)$$

The first term is due to the fact that, for $\delta s \neq 0$, the Berry-phase terms of the AF ordered components $s' \omega[\mathbf{n}] + s \sum_{i=2}^N \omega[(-1)^{i+1} \mathbf{n}] = \int d\tau (Ns\dot{\phi} + \delta s\dot{\phi}(1 + \cos\theta))$ do not add to an integer multiple of 2π .^{37,38}

Carrying out the Gaussian integral over \mathbf{l} we obtain $Z = \int \mathcal{D}\mathbf{n} \exp[-\int_0^{\beta\hbar} d\tau L[\mathbf{n}]/\hbar]$, with a Euclidean Lagrangian

$$\begin{aligned} L[\mathbf{n}] &= \frac{N\hbar^2}{8\tilde{J}} [-(\mathbf{h} + h_A n_z \mathbf{e}_z - i\mathbf{n} \times \dot{\mathbf{n}})^2 \\ &\quad + ((\mathbf{h} + h_A n_z \mathbf{e}_z) \cdot \mathbf{n})^2 - \tilde{\omega}_0^2 n_z^2] \\ &\quad + \delta s \hbar [\mathbf{h} \cdot \mathbf{n} - i\dot{\phi}(1 + \cos\theta)], \end{aligned} \quad (31)$$

where

$$\begin{aligned} \frac{\tilde{J}}{N} &= \frac{(N-2)J + 2s'J'/s}{(N + \delta s/s)^2}, \\ h_A &= \frac{2(k_z s^2 - k'_z s'^2)}{(N + \delta s/s)s\hbar}, \\ \tilde{\omega}_0^2 &= \frac{8\tilde{J}}{N} [(N-1)k_z s^2 + k'_z s'^2]. \end{aligned} \quad (32)$$

Eq. (31) is the analog of Eq. (4) for the FW. A finite excess spin δs of the modified FW leads to two significant changes in $L[\mathbf{n}]$: first, the typical energy scales of the system are slightly renormalized, $J \rightarrow \tilde{J}$ and $\omega_0 \rightarrow \tilde{\omega}_0$, even for $J' = J$ and $k'_z = k_z$. More importantly, L acquires an additional term due to the Zeeman energy

and Berry phase of the uncompensated spin $\delta s \mathbf{n}$. For all cases of experimental interest, due to Eq. (21) we have $h_A \ll \tilde{\omega}_0 \ll h_x$. The h_A -dependent terms in Eq. (31) hence lead only to minor modifications of the thermodynamic properties of the modified FW compared to the FW, but feature in the dynamics.

We will show now that, for $h_x \neq 0$, \mathbf{n} and hence the excess spin no longer trace a tunneling path in the (y, z) -plane. As can be seen from

$$L[\phi, \theta] \simeq \frac{N\hbar^2}{8\tilde{J}} [-(h_x - i\dot{\phi})^2 - \tilde{\omega}_0^2 \sin^2 \phi] - i\hbar \delta s \dot{\phi} + \frac{N\hbar^2}{8\tilde{J}} \left[\dot{\theta}^2 + \cos^2 \theta \left((h_x - i\dot{\phi})^2 + \tilde{\omega}_0^2 \sin^2 \phi \right) + 2 \cos \theta (h_x - i\dot{\phi}) \left(\delta s \frac{4\tilde{J}}{N\hbar} + h_A \sin^2 \theta \sin^2 \phi \right) \right], \quad (33)$$

the timescales for the dynamics of ϕ and θ separate due to Eq. (25), and we can again invoke the adiabatic approximation used in Sec. II B. θ oscillates in a slowly varying harmonic potential with the potential minimum at θ_0 , where

$$\cos \theta_0 = -\frac{h_x - i\dot{\phi}}{(h_x - i\dot{\phi})^2 + \tilde{\omega}_0^2 \sin^2 \phi} \left(\frac{4\tilde{J}}{N\hbar} \delta s + h_A \sin^2 \phi \right). \quad (34)$$

Corrections to the adiabatic approximation are beyond the order of the present calculation. Eq. (34) shows that finite $\delta s \neq 0$ or $h_A \neq 0$ leads to a shift in the saddle-points of the Lagrangean $L[\phi, \theta]$ away from $\theta_0 = \pi/2$, which is due to the fact that then $\mathbf{S}_A - \mathbf{S}_B$ no longer lies in the (y, z) -plane [Fig. 3c]. Expanding Eq. (33) to second order in $\vartheta = \theta - \theta_0$ and carrying out the Gaussian integral over ϑ , we obtain a ϕ -dependent effective Lagrangean

$$L[\phi] = \frac{N\hbar^2}{8\tilde{J}} [-(h_x - i\dot{\phi})^2 - \tilde{\omega}_0^2 \sin^2 \phi] - i\hbar \left(\delta s + \frac{1}{2} \right) \dot{\phi} + \hbar \frac{h_x}{2} + \mathcal{O}(\tilde{\omega}_0^2/h_x, Nh_A \tilde{\omega}_0/8\tilde{J}). \quad (35)$$

Comparison with the corresponding Lagrangean for $\delta s = 0$ [Eq. (7)] shows that, to leading order in the excess spin δs and anisotropy field h_A , the only effect of an excess spin is to introduce an additional topological phase $-i\delta s \phi$. In particular, in contrast to the case $h_x = 0$ discussed in earlier work on tunneling in ferrimagnets,^{21–24} the potential barrier and hence the real part of the tunnel action is only slightly altered by the excess spin. This is due to the fact²⁵ that, for $\hbar h_x > |\delta s| 8J/N$ [Eq. (25)], the system is in the AF regime in which the tunnel splitting is only slightly modified by the excess spin. Note that Eq. (35) is formally identical to Eq. (7), which provides a rigorous proof of the statement that the modified FW also may exhibit tunneling of \mathbf{n} for sufficiently large anisotropy, as already claimed on basis of physical arguments at the end of Sec. III.

Using the same techniques as for the FW, we find

$$Z = \exp \left[\beta \left(\frac{N\hbar^2}{8\tilde{J}} h_x^2 - \hbar \frac{h_x + \tilde{\omega}_0}{2} \right) \right] \cosh \left(\frac{\beta \tilde{\Delta}}{2} \right), \quad (36)$$

with the tunnel splitting

$$\tilde{\Delta}(h_x) = \tilde{\Delta}_0 \left| \sin \pi \left(\frac{N\hbar}{4\tilde{J}} h_x + \delta s \right) \right|, \quad (37)$$

where $\tilde{S}/\hbar = N\tilde{\omega}_0/2\tilde{J}$, $\tilde{\Delta}_0 = 8\hbar\tilde{\omega}_0\sqrt{\tilde{S}/2\pi\hbar} \exp[-\tilde{S}/\hbar]$. From Eq. (36) it is also straightforward to derive all thermodynamic quantities of interest. In particular, for the free energy F , the magnetization M_x , and the specific heat c_v we obtain

$$F = \hbar \frac{\tilde{\omega}_0 + h_x}{2} - \frac{N\hbar^2}{8\tilde{J}} h_x^2 - \frac{1}{\beta} \ln \cosh \left(\frac{\beta \tilde{\Delta}}{2} \right), \quad (38)$$

$$M_x = (g\mu_B) \left[\frac{N\hbar h_x}{4\tilde{J}} - \frac{1}{2} + \frac{1}{2\hbar} \frac{\partial \tilde{\Delta}}{\partial h_x} \tanh \left(\frac{\beta \tilde{\Delta}}{2} \right) \right], \quad (39)$$

$$c_v = k_B \left(\frac{\beta \tilde{\Delta}}{2} \right)^2 \cosh^{-2} \left(\frac{\beta \tilde{\Delta}}{2} \right). \quad (40)$$

The most significant change in the thermodynamic properties of the modified FW is that, for half-integer δs , the zeros of $\tilde{\Delta}$ and hence the magnetization steps are shifted by a magnetic field $2\tilde{J}/Ng\mu_B$, i.e. half of a magnetization plateau, compared to the unmodified wheel [Fig. 4]. The magnetization plateaus then lie at half-integer spin values. At low T , the specific heat c_v should exhibit a characteristic Schottky anomaly, with a peak at $T_0 \simeq 0.4\tilde{\Delta}/k_B$. So far, c_v has been measured only for $B_x = 0$ in Fe₁₀ and Fe₆ samples.³⁹ Measurements of T_0 in $c_v(T)$ for various $h_x \gg \tilde{\omega}_0$ would in principle allow one to observe the characteristic sinusoidal variation of $\tilde{\Delta}$ as function of h_x .

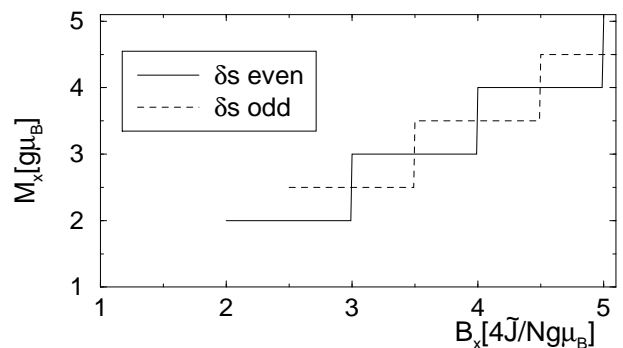


FIG. 4. Schematic plot of the ground-state magnetization of a modified FW with integer (—) and half-integer (---) δs , respectively.

The width of the magnetization plateaus, $\delta B_{c,n} = B_{c,n+1} - B_{c,n} = 4\tilde{J}/Ng\mu_B$, where $B_{c,n}$ is the field at

which the magnetization M_x exhibits the n^{th} step, is a quantity which is accessible in experiments and from which J' can be inferred. Our theory predicts

$$\delta B_{c,n}(J') - \delta B_{c,n}(J' = J) = 8 \frac{s'/s}{(N + \delta s/s)^2} \frac{(J' - J)}{g\mu_B}. \quad (41)$$

In Fig. 5 we compare the functional dependence predicted by Eq. (41) with the results of exact diagonalization (ED) on small rings, $N = 4$, $s = 2$, $s' = 3/2$ (upper panel) and $s' = 1$ (lower panel), respectively, for $|J'/J - 1| \leq 0.1$.⁴⁰ The ED results are in good agreement with the analytical result. The deviations for $|J'/J - 1| \gtrsim 0.1$ signal the breakdown of our ansatz in Eq. (26) for J' significantly different from J (see Sec. VI below).

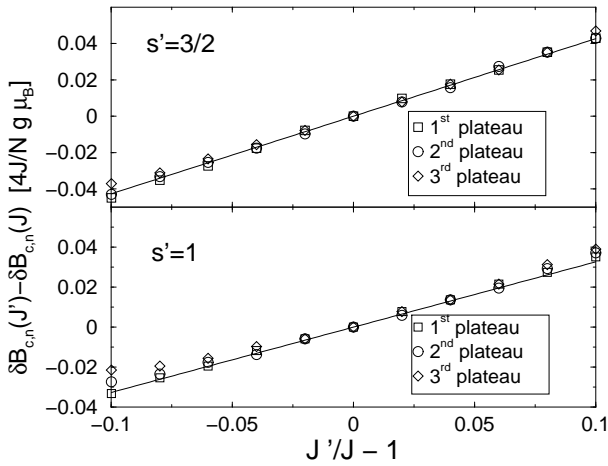


FIG. 5. Comparison of ED (symbols) and analytical (—) results for the difference in plateau width, $\delta B_{c,n}(J') - \delta B_{c,n}(J' = J)$ as function of $J' - J$ for $\delta s = -1/2$ (upper panel) and $\delta s = -1$ (lower panel). $N = 4$, $s = 2$, $k_z = k'_z = 0.1J$. The numerical error of the data points $\pm 0.002 \times 4J/Ng\mu_B$ is smaller than the symbol size.

We show now that although, for a given direction of \mathbf{n} , the total spin \mathbf{S} acquires a component perpendicular to the field \mathbf{B} , the magnetization $M_\alpha = 0$ still vanishes for $\alpha = y, z$. We define the fields $m_\alpha(\tau) = \delta \int d\tau L[\mathbf{n}] / \delta(\hbar h_\alpha(\tau))|_{h_\alpha \equiv 0}$ such that $M_\alpha = -(g\mu_B) \int \mathcal{D}\mathbf{n} m_\alpha(\tau) e^{-\int d\tau L/\hbar} / Z$. Using Eq. (33), we obtain

$$\begin{aligned} m_z &= \frac{N\hbar}{4\tilde{J}} [-h_A n_z (1 - n_z^2) \\ &\quad + h_x n_x n_z + i(\mathbf{n} \times \dot{\mathbf{n}})_z] + \delta s n_z \\ &\simeq -\frac{N\hbar}{4\tilde{J}} h_A \sin \phi + \delta s \frac{\tilde{\omega}_0^2}{(h_x - i\dot{\phi})^2} \sin^3 \phi \\ &\quad + i \frac{N\hbar}{4\tilde{J}} \dot{\theta}_0 \cos \phi + \mathcal{O}(\vartheta), \end{aligned} \quad (42)$$

with θ_0 defined in Eq. (34).⁴¹ As follows from the invariance of \hat{H} under rotation around \mathbf{B} by π , $M_y = M_z = 0$

for arbitrary h_x . In particular, at $T = 0$, $M_z = 0$ indicates that the ground-state is not a state with definite direction of \mathbf{n} , but rather a coherent superposition of such states, $(|\uparrow\rangle + |\downarrow\rangle)/\sqrt{2}$, as expected for a system which shows coherent Néel vector tunneling.

V. DYNAMICS OF THE MODIFIED FW

As we have shown above, the effective action $L[\phi]$ of the modified FW [Eq. (35)] is formally identical to that of the FW [Eq. (7)]. In particular, for large anisotropy k_z , such that $\tilde{S}/\hbar \gg 1$, the modified FW is in the quantum tunneling regime [Sec. II A]. In this section, we evaluate explicitly the spin susceptibility $\chi_{zz}(\tau)$ for the modified FW.

In order to motivate this, we first calculate χ_{zz} using the results of the classical vector model [Sec. III]. For \mathbf{n} along \mathbf{e}_z or $-\mathbf{e}_z$, the z -component of the total spin vector is finite, $S_z = \pm S_0$, where $S_0 = \delta s \omega_0^2 / h_x^2 + (k'_z s'^2 - k_z s^2) / 2Js$. For $\mathbf{n}(t = 0) = \mathbf{e}_z$, the coherent tunneling of \mathbf{n} then results in an oscillating $S_z(t) = S_0 \cos(\tilde{\Delta}t/\hbar)$, such that the Fourier transform of the (real-time) susceptibility exhibits an absorption pole $\chi''_{zz}(\omega \simeq \tilde{\Delta}/\hbar) = \pi |S_0|^2 \tanh(\beta\tilde{\Delta}/2) \delta(\omega - \tilde{\Delta}/\hbar)$.

Generalizing the procedure for the FW [Appendix A] to $\delta s \neq 0$, we calculate the quantum corrections to this result from⁴²

$$\begin{aligned} \chi_{zz}(\tau) &= (g\mu_B)^2 \frac{N\hbar}{4\tilde{J}} (1 - \langle \sin^2 \phi \rangle) \delta(\tau) \\ &\quad + (g\mu_B)^2 \frac{1}{Z} \int \mathcal{D}\mathbf{n} e^{-\int_0^{\beta\hbar} d\tau L[\mathbf{n}]/\hbar} m_z(\tau) m_z(0), \end{aligned} \quad (43)$$

with $m_z(\tau)$ given in Eq. (42). As for the undoped FW, the correlations of the ϑ -terms in $m_z(\tau)$ give rise to a strongly peaked term $(g\mu_B)^2 N\hbar \delta(\tau) \langle \sin^2 \phi \rangle / 4\tilde{J}$. We hence find⁴³

$$\begin{aligned} \chi_{zz}(\tau) &= (g\mu_B)^2 \frac{N\hbar}{4\tilde{J}} \delta(\tau) \\ &\quad + (g\mu_B)^2 \frac{1}{Z} \int \mathcal{D}\phi e^{-\int_0^{\beta\hbar} d\tau L[\phi]/\hbar} \left(-\frac{N\hbar h_A}{4\tilde{J}} \sin \phi(\tau) \right. \\ &\quad \left. + \delta s \frac{\tilde{\omega}_0^2}{h_x^2} \sin^3 \phi(\tau) \right) \left(-\frac{N\hbar h_A}{4\tilde{J}} \sin \phi + \delta s \frac{\tilde{\omega}_0^2}{h_x^2} \sin^3 \phi \right). \end{aligned} \quad (44)$$

In stark contrast to the FW, the path integral in Eq. (44) gives rise to terms proportional to $\exp[\pm \tilde{\Delta}|\tau|/\hbar]$ such that, upon Fourier transform, the susceptibility in Matsubara representation contains terms $1/(i\omega_n \pm \tilde{\Delta}/\hbar)$. The path integral is most easily evaluated in a Hamiltonian description. We quantize the field ϕ and use an effective two-state Hamiltonian to evaluate the matrix elements. Inserting the expression for h_A , we find [Appendix B]

$$|\langle e | \hat{S}_z | g \rangle| = \left| \frac{N(k'_z s'^2 - k_z s^2)}{2\tilde{J}s(N + \delta s/s)} \left(1 - \frac{\tilde{J}}{N\hbar\tilde{\omega}_0} \right) \right|$$

$$+\delta s \frac{\tilde{\omega}_0^2}{h_x^2} \left(1 - 3 \frac{\tilde{J}}{N\hbar\tilde{\omega}_0} \right), \quad (45)$$

$$\chi''_{zz}(\omega \simeq \tilde{\Delta}) = \pi(g\mu_B)^2 |\langle e|\hat{S}_z|g\rangle|^2 \times \tanh\left(\frac{\beta\tilde{\Delta}}{2}\right) \delta(\omega - \tilde{\Delta}/\hbar). \quad (46)$$

Eqs. (45) and (46) are the main results of this section. For $\delta s = -5/2$ or -1 (for Ga and Cr dopants, respectively), $|\langle e|\hat{S}_z|g\rangle|$ can be of order 0.1 even for $h_x \gtrsim 3\tilde{\omega}_0$. For $k_B T \lesssim \tilde{\Delta}$ the susceptibility of the modified FW then exhibits a resonance at $\omega = \pm\tilde{\Delta}/\hbar$ which is accessible in AC susceptibility or ESR measurements. The terms $\tilde{J}/N\hbar\tilde{\omega}_0 = 1/(2\tilde{S}/\hbar)$ in $|\langle e|S_z|g\rangle|$ are quantum corrections to the classical result derived at the beginning of this section.

So far we have ignored decoherence of the spin tunneling, which is crucial for the notion of MQC. The condition $\Gamma \simeq \tilde{\Delta}/\hbar$, where Γ is the electron spin decoherence rate, marks the transition from coherent to incoherent tunneling dynamics. As is evident from the classical vector model discussed in Sec. III, S_z follows the tunneling dynamics of \mathbf{n} . In particular, for a single modified FW, the decay rate of $|\langle n_z(t)n_z \rangle|$, Γ , is also the decay rate of $|\langle S_z(t)S_z \rangle|$. For $\Gamma \neq 0$, the δ -peak in Eq. (46) is then broadened into a Lorentzian of width Γ . In experiments carried out on an ensemble of modified FWs, inhomogeneous broadening (e.g. due to crystal defects or nuclear spins) adds to the width of the resonance peaks. The experimentally determined linewidth of the absorption and emission peaks provides an upper limit for Γ . This should allow one to settle the experimentally unresolved problem of whether true quantum coherence is established in ferric wheels.

Finally we compare our result for the transition matrix element $|\langle e|S_z|g\rangle|$ entering Eq. (46) with results obtained from ED on small rings for a wide range of parameters [Figs. 6, 7, 8]. For simplicity, we assume $J' = J$. In the range of validity of our theory [Eq. (25)], for $\delta s \neq 0$ [Figs. 6, 8], the agreement of ED (\diamond) with analytic results (—) is both qualitatively and quantitatively convincing.⁴⁴ The small oscillating features seen in the exact results are due to tunneling corrections $\mathcal{O}(\exp[-\tilde{S}/\hbar])$ to $|\langle e|S_z|g\rangle|$, which were neglected in Eq. (45). For Fig. 7, where $\delta s = 0$, our theory makes the correct qualitative prediction that $|\langle e|S_z|g\rangle|$ depends only weakly on h_x , but overestimates the matrix element. However, due to the smallness of the matrix element for $\delta s = 0$, the discrepancy can be due to terms neglected in the derivation of Eq. (35). The significantly different qualitative features of Fig. 7 compared to Figs. 6 and 8 arise from the fact that $\delta s = 0$ in Fig. 7. The different functional dependence of $|\langle e|S_z|g\rangle|$ on h_x for the two cases $\delta s \neq 0$ and $\delta s = 0$ is well understood within the theoretical framework presented here [Eq. (45)]. The very large difference in matrix element magnitude illustrates the importance of looking at doped rings in experiment.

We conclude this section by remarking that, for finite excess spin δs , the second transverse susceptibility $\chi''_{yy}(\omega)$ also has an absorption pole at $\omega = \tilde{\Delta}/\hbar$. However, since \mathbf{e}_y is a hard axis, the spectral weight of this pole is significantly smaller than that of $\chi''_{zz}(\omega)$, such that Néel vector tunneling in the modified FWs can be more easily detected by probing the latter quantity.

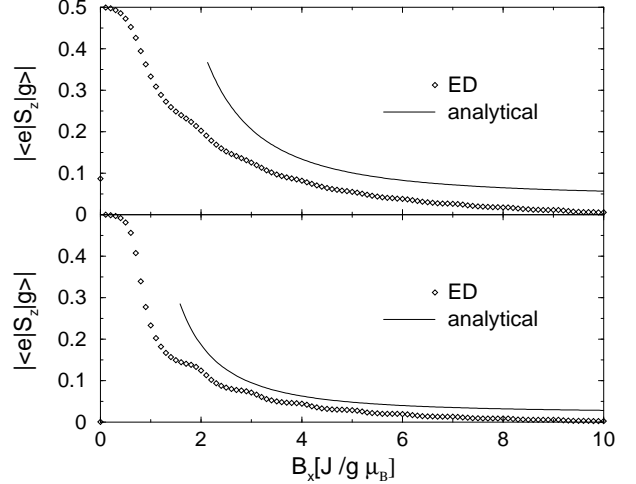


FIG. 6. Transition matrix element $|\langle e|S_z|g\rangle|$ for small rings, $N = 4$ with $J' = J$, $s = 5/2$, $s' = 2$. In the upper panel, $k_z = k'_z = 0.1$. In the lower panel, $k_z = k'_z = 0.055J$ is chosen such that $\tilde{S}/\hbar \simeq 3.3$ as for Fe₁₀. The analytical result (—) is shown for $\max[\hbar\tilde{\omega}_0, |\delta s|8J/N] < \hbar h_x < 4Js$. Due to Eq. (25), our theory is rigorously valid only for fields much larger than $\max[\hbar\tilde{\omega}_0, |\delta s|8J/N]$ and much smaller than $4Js$.

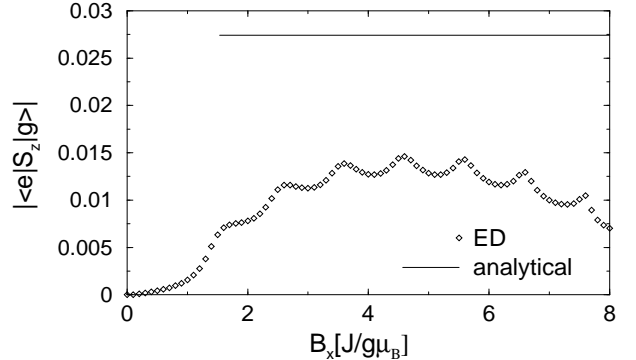


FIG. 7. Transition matrix element $|\langle e|S_z|g\rangle|$ for a small ring $N = 4$ with $J' = J$, $s = s' = 2$, i.e. $\delta s = 0$, but $k'_z = 1.5k_z$ and hence $h_A \neq 0$. Again, $k_z = 0.0655J$ is chosen such that $\tilde{S}/\hbar \simeq 3.3$, as for Fe₁₀. The analytical result (—) is shown for $\max[\hbar\tilde{\omega}_0, |\delta s|8J/N] < \hbar h_x < 4Js$. See also caption of Fig. 6.

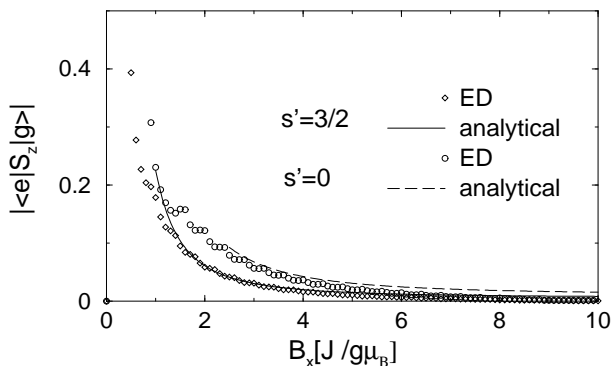


FIG. 8. Transition matrix element $|\langle e|S_z|g\rangle|$ obtained with the phenomenological sublattice Hamiltonian [Eq. (19)] for Fe_{10} with one $s = 5/2$ substituted by (a) a dopant with $s' = 3/2$ (e.g. Cr) (numerical data \diamond , analytical prediction —), and (b) a dopant with $s' = 0$ (e.g. Ga) (numerical data \circ , analytical prediction - -). Note that, in this case, the numerical data is not obtained from ED of Eq. (1), but rather of Eq. (19). For simplicity, we assumed $J' = J$ and $k'_z = k_z = 0.0088J$. The analytical results (— and - -) are shown for $\max[\hbar\tilde{\omega}_0, |\delta s|8J/N] < \hbar h_x < 4Js$. See also caption of Fig. 6.

VI. THERMODYNAMICS AND SPIN DYNAMICS FOR $J'/J \gg 1$ AND $J'/J \ll 1$

The deviations of the ED results from our theoretical predictions shown in Fig. 5 indicate that, for $J'/J \ll 1$ or $J'/J \gg 1$, the theory developed in Sec. IV is no longer immediately applicable. Indeed, results obtained by ED for the ground-state magnetization M_x in small rings ($N = 4$, $s = 2$, and $s' = 3/2$) [Fig. 9] indicate that one of the main results of Sec. IV, that M_x exhibits a series of equally spaced magnetization steps, does not hold any more. As we will show below, this is due to the fact that our ansatz Eq. (26) needs to be modified for J' significantly different from J . In this section we show that, for the limiting cases of $J' \gg J$ or $J' \ll J$, the modified FW can be mapped onto the problem discussed in the preceding sections. We discuss the qualitative features of M_x for these systems and show that coherent tunneling of \mathbf{n} also results in coherent oscillations of the total spin.

$J' \ll J$: In this limit, \mathbf{s}_1 decouples from all other spins and aligns antiparallel to \mathbf{B} for $\hbar h_x \gtrsim J's$. The remaining spins $\mathbf{s}_2, \mathbf{s}_3, \dots, \mathbf{s}_N$ form an open spin chain, as sketched in Fig. 10a. As shown in Appendix C, the Lagrangean of an open spin chain with an odd number of spins can also be mapped onto Eq. (35), with $\delta s = s$ and slightly renormalized $\tilde{J} = JN(N-2)/(N-1)^2$. We predict that M_x has the following features:

- $M_x \gtrsim g\mu_B(s' + s)$ for $2J's \ll \hbar h_x$.
- For $\max[\hbar\tilde{\omega}_0, s8\tilde{J}/N] \ll \hbar h_x \ll 4\tilde{J}s$, M_x exhibits a series of equally spaced magnetization steps with plateau width $\delta B_{c,n} = 4\tilde{J}/Ng\mu_B$. Depending on

whether δs is half-integer or integer, the plateaus correspond to states with half-integer or integer total spin, respectively.

$J' \gg J$: In this limit, the spins $\mathbf{s}_N, \mathbf{s}_1$ and \mathbf{s}_2 are strongly coupled. In a semiclassical picture, \mathbf{s}_1 aligns antiparallel to \mathbf{s}_N and \mathbf{s}_2 and the three spins act as one single spin $|2s - s'|$ coupled to \mathbf{s}_3 and \mathbf{s}_{N-2} with exchange constant J [Fig. 10b]. For simplicity we assume $s' < 2s$. Then, for $\hbar h_x \ll J'(s - \delta s + 1)$, \hat{H} can be mapped onto a Hamiltonian of the form Eq. (1) with $N \rightarrow N-2$, $J' \rightarrow J$, $k'_z \rightarrow (k'_z s'^2 + 2k_z s^2)/(2s - s')^2$, and $s' \rightarrow 2s - s' = s - \delta s$. Because all $N - 2$ exchange couplings in the new Hamiltonian are identical, the theory developed in Sec. IV and V remains applicable. In particular, for the ground-state magnetization M_x we make the following predictions:

- For $\max[\hbar\tilde{\omega}_0, |\delta s|8J/(N-2)] \ll \hbar h_x \ll 4Js$, M_x exhibits a series of equally spaced magnetization steps with $\delta B_{c,n} \simeq 4J/(N-2)g\mu_B$. Depending on whether δs is half-integer or integer, the plateaus correspond to states with half-integer or integer total spin, respectively.
- For $\hbar h_x \gtrsim J'(s - \delta s + 1)$, the Zeeman energy is sufficiently large to destroy the AF configuration of $\mathbf{s}_N, \mathbf{s}_1$, and \mathbf{s}_2 . This results in a series of additional magnetization steps with spacing J' .

Note that a similar argument also applies if $J' < 0$. In this case, the three spins $\mathbf{s}_N, \mathbf{s}_1$, and \mathbf{s}_2 are ferromagnetically coupled and align parallel. Again, the system can be mapped onto a smaller ring (as in Fig. 10b), where now $s' \rightarrow 2s + s'$. The magnetization curve resembles the one shown in the upper panel of Fig. 9. In Fig. 9, ED results for small rings with $N = 4$, $s = 2$, $s' = 3/2$ are displayed. The qualitative features agree with all the above predictions.

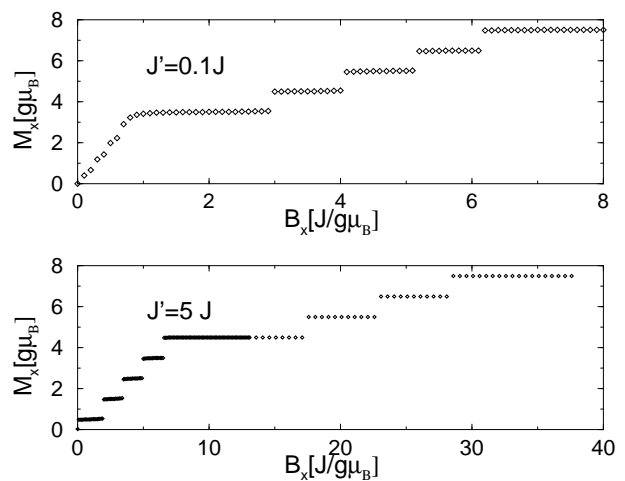


FIG. 9. $M_x(B_x)$ at $T = 0$ for a small system with $J' \ll J$ (upper panel) or $J' \gg J$ (lower panel). Here, $N = 4$, $s = 2$, $s' = 3/2$, $k_z = k'_z = 0.1$.

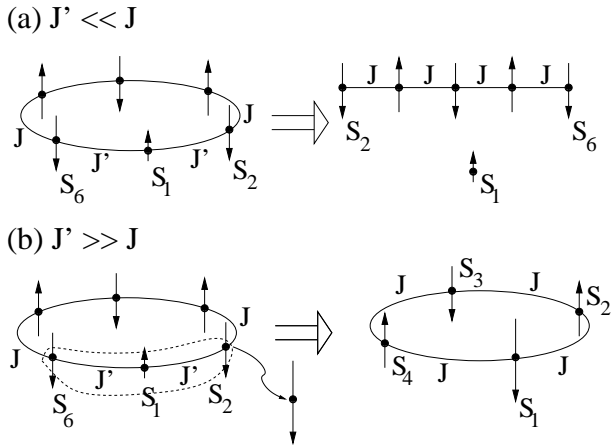


FIG. 10. (a) For $J' \ll J$, \mathbf{s}_1 decouples from all other spins and the modified FW can be mapped onto an open spin chain excluding \mathbf{s}_1 . (b) For $J' \gg J$, \mathbf{s}_N , \mathbf{s}_1 , and \mathbf{s}_2 are strongly coupled such that they can be described as one single large spin. The Hamiltonian of the ring then maps onto that of a modified FW with $J' = J$.

We conclude that even the qualitative features of M_x allow one to estimate the parameter J' of a modified FW. Even more important, as we have shown, also for $J' \ll J$ and $J' \gg J$ the modified FW can be mapped onto the Lagrangean [Eq. (31)] of a system which exhibits quantum tunneling of \mathbf{n} . In all cases discussed above, the quantum tunneling of \mathbf{n} leads to coherent oscillations of the total spin \mathbf{S} , and thus can be observed in AC susceptibility or ESR measurements.

VII. DISCUSSION

The theory described in Secs. IV, V, and VI allowed us to derive explicit expressions for both thermodynamic quantities [Eqs. (39) and (40)] and the susceptibility χ''_{zz} [Eqs. (45) and (46)] of modified FWs. In order to establish a connection with experimental issues, we now outline the steps necessary to detect coherent Néel vector tunneling. For simplicity we restrict our considerations to Fe_{10} with Ga ($\delta s = -5/2$) or Cr ($\delta s = -1$) impurity ions, and assume $J' \simeq J$.

For finite excess spin δs , the two energetically degenerate spin configurations [Fig. 1] required for coherent spin tunneling as discussed in the present work certainly exist if $\hbar h_x \gg |\delta s| 8J/N$ [Eq. (25)]. This tunneling regime is well within experimental reach for Cr dopants ($B_x \gg 9\text{T}$), but not for Ga dopants ($B_x \gg 23\text{T}$).⁴⁵ For Cr dopants ($s' \neq 0$), however, the two new parameters J' and k'_z introduced in \hat{H} [Eq. (1)] must first be determined in order to characterize the ring system.

Both J' and k'_z can be obtained from the measurement of two independent thermodynamic quantities, such as the ground-state magnetization and tunnel splitting. A schematic plot of the ground-state magnetization for integer δs (o) is shown in Fig. 4. Although the mag-

netization steps are smeared out at finite temperature, for $T \lesssim 1\text{K}$, the magnetization step spacing $\delta B_{c,n}$ still can be obtained with high accuracy.¹⁰ With $\delta B_{c,n} = 4\tilde{J}/Ng\mu_B$ and Eq. (32), this allows one to determine J' . The on-site anisotropy k'_z can be obtained from $\tilde{\Delta}$, which depends sensitively on the tunnel action $\tilde{S} \propto \sqrt{(N-1)k_z s^2 + k'_z s'^2}$ and hence on k'_z . The tunnel splitting $\tilde{\Delta}$ (and hence k'_z) is accessible either in AC susceptibility or ESR measurements [Eq. (46)], or in measurements of thermodynamic quantities, such as c_v . Torque magnetometry is another experimental technique which has been used to determine the anisotropy constant with quasi-spectroscopic accuracy.³¹

Once J' and k'_z are known, Eq. (46) determines both the position and the spectral weight of the resonance in $\chi''_{zz}(\omega)$ which arises from coherent quantum tunneling of \mathbf{n} . The characteristic functional dependence of $\tilde{\Delta}$ [Eq. (37)] and $|\langle e|S_z|g\rangle|^2$ [Eq. (45)] on h_x predicted by our theory can be checked experimentally. Finally, it is noteworthy that, although $\tilde{\Delta}$ can be determined from thermodynamic quantities, the key problem of MQC is the measurement of the decoherence rate Γ which is accessible only in dynamic quantities, such as AC susceptibilities.

Throughout the current work, we have considered FWs with only one dopant ion. As we have shown in the preceding sections, thermodynamic and dynamic quantities of doped FWs may differ significantly from those of undoped FWs. In the large samples investigated experimentally, doping will lead to a random distribution both of the number of dopant ions and of their position relative to the direction of the magnetic field. We defer a detailed analysis of these issues to a future publication. Here we note only that the random distribution of impurities does not invalidate the above considerations, and stress the qualitative features which ensure this. The choice of a low impurity concentration results in a large majority of the FWs containing no dopants or having only one dopant ion, which allows one to extract the system parameters of the singly doped FWs. When intraring dipolar interactions make a significant contribution to the effective uniaxial anisotropy k_z , doping with only one ion changes the effective anisotropy from uniaxial to biaxial. The theoretical framework presented in this paper can be readily extended to account for biaxial anisotropies. Because the original uniaxial anisotropy dominates the biaxial correction, the altered tunnel splittings $\tilde{\Delta}_i$ in a singly doped FW have a magnitude similar to $\tilde{\Delta}$ for the undoped FW, and a separation which is small by comparison. Thus AC susceptibility or ESR measurements can be expected to observe signals corresponding to reversals of the total spin accompanying Néel vector tunneling, and governed by the frequencies $\tilde{\Delta}_i$.

VIII. SPIN QUANTUM TUNNELING IN FERRITIN

The theoretical framework developed in this work is quite general and applies to other systems besides AF ring systems. In particular, the results of the classical sublattice model [Sec. III] can be easily extended to different systems. In order to illustrate this point, we now discuss natural horse-spleen ferritin and artificial magnetoferritin, in which spin quantum tunneling has already been studied experimentally^{18–20} and theoretically.^{22–25,46} The experiments were carried out in the presence of small static magnetic fields ($B_x \lesssim 10^{-6}\text{T}$). In this regime, $B_x \neq 0$ leads to an energy bias between the states $|\uparrow\rangle$ and $|\downarrow\rangle$, and tunneling is suppressed for increasing B_x .

Recently it was shown²⁵ that, for sufficiently large field, i.e. $\hbar h_x \sim |\delta s| 8J/N$, there are again two energetically degenerate spin configurations between which spin quantum tunneling may take place. In natural horse-spleen ferritin,⁴⁶ $J \simeq 200\text{K}$ and $\delta s/N \simeq 0.05$. For a system with uniaxial hard axis anisotropy, $\hat{H}_{an,z} = k_z \sum_i \hat{s}_{i,z}^2$, the tunnel barrier and hence the tunnel action can be effectively controlled over a wide range of parameters by varying the magnetic field B_x applied in the easy plane.²⁵ Tunneling in the plane perpendicular to \mathbf{B} gives rise to a topological phase acquired by the spins.^{47,48,6} A drawback of the setup considered in Ref. 25 is that, for uniaxial hard axis anisotropy, spin tunneling leaves the total spin \mathbf{S} invariant if \mathbf{B} is applied perpendicular to the hard axis. As for the FW with equal sublattice spins, spin tunneling cannot be observed in AC susceptibility measurements.

However, experiments indicate that, in addition to the strong hard-axis anisotropy, ferritin also exhibits a second weak hard-axis anisotropy $\hat{H}_{an,y} = k_y \sum_i \hat{s}_{i,y}^2$, where⁴⁶ $k_y/k_z \simeq 10^{-3}$. In self-sustaining films of natural horse-spleen ferritin, the hard axis \mathbf{e}_z is perpendicular to the film.²⁰ In the simplest experimental setup, interference of different spin tunnel paths then could be explored if a field $\mathbf{B} = B_z \mathbf{e}_z$ is applied along the hard axis. As long as $\hbar h_z \ll Nk_z s^2/\delta s$ ($\simeq 10\text{K}$ for horse-spleen ferritin), due to the large anisotropy energy the spins remain confined to the film plane such that there are again two energetically degenerate spin configurations similar to Fig. 1. Tunneling takes place in the plane perpendicular to \mathbf{B} , with a tunnel splitting

$$\Delta = \Delta_0 \left| \cos \pi \left(S_{\text{tot}} + \frac{N\hbar}{4J} h_z \right) \right|, \quad (47)$$

where $\Delta_0 \simeq 5 \times 10^{-5}\text{K}$ and the total staggered spin is $S_{\text{tot}} \simeq 2.5 \times 4500$ for natural horse-spleen ferritin. Δ is periodic as a function of B_z , with a period $\delta B_z = 4J/Ng\mu_B$ ($\simeq 0.13\text{T}$ for natural horse-spleen ferritin). The advantage of this tunnel scenario is that quantum tunneling of \mathbf{n} also results in a tunneling of the excess

spin δs , and hence leads to a large resonance peak in the susceptibility per ferritin molecule, i.e.

$$\chi''_{xx}(\omega \simeq \Delta/\hbar) \simeq \frac{1}{2} \pi (\delta s)^2 \tanh \left(\frac{\beta \Delta}{2} \right) \delta(\omega - \Delta/\hbar). \quad (48)$$

The factor 1/2 takes into account the random distribution of easy axes in the film plane. Due to the spread in particle number, the total staggered spin of the system can be either integer or half-integer. Hence, one will observe two different tunnel splittings varying with h_z as $\Delta = \Delta_0 |\cos(\pi N \hbar h_z / 4J)|$ and $\Delta = \Delta_0 |\sin(\pi N \hbar h_z / 4J)|$. An experimental confirmation of this behavior would provide further strong evidence that the resonance observed in AC susceptibility measurements in ferritin^{18–20} is due to macroscopic spin tunneling. In particular, the period of the oscillations of Δ as function of the applied field B_z would allow one to estimate the total number of tunneling spins.

IX. CONCLUSION

The AF ring systems discussed here, modified ferric wheels which are already available to experimentalists, combine the advantages of AF and ferromagnetic molecular magnets. The tunnel splitting $\hat{\Delta}$ is sufficiently large that quantum coherence between macroscopically different states is established. Tunneling of the Néel vector \mathbf{n} also leads to a tunneling of the total spin \mathbf{S} , thus making the spin dynamics in modified FWs accessible to experiment. We have considered the simplest realistic model Hamiltonian \hat{H} [Eq. (1)] for a system in which, for example, one of the Fe ions is exchanged by Cr or Ga. We showed that the additional parameters entering \hat{H} can be inferred from equilibrium quantities such as the magnetization. Moreover, for a wide range of parameters, the system still exhibits MQC in the form of coherent tunneling of \mathbf{n} . Finally, we calculated spin correlation functions of the modified FW and showed that tunneling of \mathbf{n} can indeed be observed in AC susceptibility or ESR experiments, which allow one to measure both the tunnel splitting $\hat{\Delta}$ and an upper bound for the spin decoherence rate Γ . Hence they should be appropriate to verify experimentally that Néel vector tunneling in FWs is coherent.

Throughout this work we have used spin coherent-state path integrals leading to a NLSM-description for the modified FW. The main advantage of this technique over ED is that thermodynamic and dynamic quantities can be evaluated for a realistic system size. In addition, an intuitive physical understanding of the spin dynamics (quantum tunneling of \mathbf{n}) can be obtained. A drawback of the analytical approach chosen in the present work is that it naturally requires approximations. Corrections to our results, in particular 1/s-corrections, may become

appreciable for the parameters of the FWs. However, our analytical results for $|\langle e|\hat{S}_z|g\rangle|$ agree well with ED results obtained for small systems. For the parameter range explored in ED, deviations from our theoretical predictions become significant mainly if s' is small ($s' = 1/2$ or 1), where the ansatz Eq. (26) fails due to large quantum fluctuations of $\hat{\mathbf{s}}_1$. Although numerical work on rings with $N = 6, 8,$ and 10 is challenging, some results have been obtained for the ground-state magnetization and torque.¹⁵ A detailed numerical study also of spin correlation functions would provide clearer evidence for the range of validity of the present approach and could explore its limitations. For example, as is well known, the sublattice Hamiltonian Eq. (18) is exact for $N = 4$. For increasing N , however, ED results⁴⁹ show that there are small deviations from $\hat{H}_{0,\text{subl}}$.

Note that our work also has important implications for undoped ferric wheels. Recent torque,⁵⁰ c_v ,⁵⁰ and proton $1/T_1$ -measurements⁵¹ on single crystals of various Fe_6 compounds indicate that these FWs could exhibit physics beyond the Hamiltonian Eq. (2). One important future step in explaining the new experimental data will be to clarify to which extent the observed phenomena can be attributed to inhomogeneous level broadening. The theoretical framework presented here allows one to calculate analytically the inhomogeneous level broadening resulting from a random distribution of single exchange couplings J' and on-site anisotropies k'_z which could be a consequence of lattice defects in Fe_6 crystals. Indeed, recent work on Mn_{12} suggests that lattice distortions⁵² and a distribution of anisotropy energies and g -factors^{53,54} could account for the observed broad distribution of tunneling rates in Mn_{12} .

Finally, we stress once more that the Hamiltonian \hat{H} [Eq. (1)] discussed in this paper is a simple model Hamiltonian, which still leads to fascinating novel features in the physical properties of the modified FWs. However, as discussed in Sec. VII, realistic systems might require modification of Eq. (1). Generalization of the present approach to more complicated anisotropies is, however, straightforward.

ACKNOWLEDGMENTS

This work was supported in part by the European Network MolNanoMag under grant number HPRN-CT-1999-00012, by the Federal Office for Education and Science (BBW) Bern, and by the Swiss National Fund. We are indebted to F. Borsa, A. Cornia, V. Golovach, A. Honacker, A. Lascialfari, M. Leuenberger, and in particular B. Normand for stimulating discussions.

APPENDIX A: SUSCEPTIBILITIES

In this appendix, we sketch how the transverse susceptibilities $\chi_{\alpha\alpha}(i\omega_n)$, $\alpha = y, z$, can be evaluated for the FW with Hamiltonian \hat{H}_0 [Eq. (2)]. With $M_y = M_z = 0$,⁴²

$$\begin{aligned} \chi_{\alpha\alpha}(\tau) &= (g\mu_B)^2 \frac{N\hbar}{4J} \delta(\tau) (1 - \langle n_\alpha^2 \rangle) \\ &+ (g\mu_B)^2 \left(\frac{N\hbar}{4J} \right)^2 \frac{1}{Z} \int \mathcal{D}\mathbf{n} [i(\mathbf{n} \times \dot{\mathbf{n}})_\alpha + n_\alpha h_x n_x]_\tau \\ &\quad [i(\mathbf{n} \times \dot{\mathbf{n}})_\alpha + n_\alpha h_x n_x]_0 e^{-\int_0^{\beta\hbar} d\tau L_0[\mathbf{n}]/\hbar}, \quad (\text{A1}) \end{aligned}$$

where the first (second) square bracket is evaluated at τ (0). Using the parameterization in Eq. (5) and expanding to second order in $\vartheta = \theta - \pi/2$, for $\alpha = y$ the square bracket reads

$$i(\mathbf{n} \times \dot{\mathbf{n}})_y + n_y h_x n_x = -(h_x - i\dot{\phi})\vartheta \cos \phi - i\dot{\vartheta} \sin \phi. \quad (\text{A2})$$

The corresponding expression for $\alpha = z$ can be obtained by setting $\phi \rightarrow \phi - \pi/2$. Integrating ϑ , we obtain

$$\begin{aligned} \chi_{yy}(\tau) &= (g\mu_B)^2 \frac{N\hbar}{4J} (1 - \langle \cos^2 \phi \rangle) \delta(\tau) \\ &+ \left(\frac{N\hbar}{4J} \right)^2 \frac{1}{Z} \int \mathcal{D}\phi e^{-\int_0^{\beta\hbar} d\tau L_0[\phi]/\hbar} \\ &\quad \times [G_{\vartheta\vartheta}(\tau)(h_x - i\dot{\phi}(\tau)) \cos \phi(\tau) (h_x - i\dot{\phi}) \cos \phi \\ &\quad + iG_{\vartheta\dot{\phi}}(\tau)(h_x - i\dot{\phi}(\tau)) \cos \phi(\tau) \sin \phi \\ &\quad + iG_{\dot{\phi}\vartheta}(\tau) \sin \phi(\tau)(h_x - i\dot{\phi}) \cos \phi \\ &\quad + i^2 G_{\dot{\phi}\dot{\phi}}(\tau) \sin \phi(\tau) \sin \phi]. \quad (\text{A3}) \end{aligned}$$

The Green functions are defined by $G_{\vartheta\vartheta}(\tau) = \langle T_\tau \vartheta(\tau) \vartheta \rangle - \langle \vartheta \rangle^2$. In the high-field limit $h_x \gg \omega_0$, all Green functions are strongly peaked at $\tau = 0$. Using the adiabatic approximation outlined in Sec. II A, we find from $L_0[\mathbf{n}]$ [Eq. (6)] (up to $\mathcal{O}(\omega_0^2/h_x^2)$)

$$G_{\vartheta\vartheta}(\tau) \simeq \frac{2J}{N\hbar(h_x - i\dot{\phi})} e^{-(h_x - i\dot{\phi})|\tau|}, \quad (\text{A4})$$

$$G_{\vartheta\dot{\phi}}(\tau) \simeq \frac{2J}{N\hbar} \text{sgn}(\tau) e^{-(h_x - i\dot{\phi})|\tau|}, \quad (\text{A5})$$

$$G_{\dot{\phi}\dot{\phi}}(\tau) \simeq \frac{4J}{N\hbar} \delta(\tau) - \frac{2J(h_x - i\dot{\phi})}{N\hbar} e^{-(h_x - i\dot{\phi})|\tau|}, \quad (\text{A6})$$

where $\dot{\phi} = \dot{\phi}(0)$. Along the classical path, the field ϕ varies on a timescale $1/\omega_0$, i.e. slowly on the timescale over which the Green functions vanish, which allows us to set $\exp[-(h_x - i\dot{\phi})|\tau|] \rightarrow (2/(h_x - i\dot{\phi}))\delta(\tau)$ in $G_{\vartheta\vartheta}$ and $G_{\dot{\phi}\dot{\phi}}$. Because $G_{\vartheta\dot{\phi}} = -G_{\dot{\phi}\vartheta}$ the second and third term in Eq. (A3) cancel. To leading order in ω_0/h_x we then obtain

$$\chi_{yy}(\tau) \simeq (g\mu_B)^2 \frac{N\hbar}{4J} \left[(1 - \langle \cos^2 \phi + \sin^2 \phi \rangle) \delta(\tau) \right]$$

$$\begin{aligned}
& + \frac{h_x}{2} e^{-h_x|\tau|} \Big] \\
= (g\mu_B)^2 \frac{N\hbar h_x}{8J} e^{-h_x|\tau|} & \simeq (g\mu_B)^2 \frac{N\hbar}{4J} \delta(\tau), \quad (\text{A7})
\end{aligned}$$

and

$$\chi_{zz}(\tau) \simeq (g\mu_B)^2 \frac{N\hbar h_x}{8J} e^{-h_x|\tau|} \simeq (g\mu_B)^2 \frac{N\hbar}{4J} \delta(\tau). \quad (\text{A8})$$

APPENDIX B: TWO-STATE MODEL OF THE MODIFIED FW

As shown in Secs. I and II, for weak tunneling $\tilde{\mathcal{S}}/\hbar \gg 1$, the low-energy sector of the (modified) FW can be described as a two-state model with basis $|\uparrow\rangle$ and $|\downarrow\rangle$. In this approximation, $\hat{H} = -(\tilde{\Delta}/2)[|\uparrow\rangle\langle\downarrow| + |\downarrow\rangle\langle\uparrow|]$, where the parameters of the original microscopic Hamiltonian enter $\tilde{\Delta}$.

For any operator \hat{O} , the transition matrix element between $|g\rangle$ and $|e\rangle$ can be evaluated from

$$\begin{aligned}
\langle e|\hat{O}|g\rangle &= \frac{1}{2} \left(\langle \uparrow|\hat{O}|\uparrow\rangle - \langle \downarrow|\hat{O}|\downarrow\rangle \right. \\
& \left. + \langle \uparrow|\hat{O}|\downarrow\rangle - \langle \downarrow|\hat{O}|\uparrow\rangle \right). \quad (\text{B1})
\end{aligned}$$

For $h_x \gg \tilde{\omega}_0$ the state $|\uparrow\rangle$ describes a Gaussian probability distribution for \mathbf{n} in the plane $\perp \mathbf{B}$ with variance $\langle \uparrow|\cos^2\phi|\uparrow\rangle = 2\tilde{J}/N\hbar\tilde{\omega}_0 = 1/(\tilde{\mathcal{S}}/\hbar)$ [Sec. II A]. Expanding $\sin\phi \simeq \pm(1 - \cos^2\phi/2)$ for $\phi \simeq \pi/2$ and $\phi \simeq 3\pi/2$, respectively, we obtain

$$\begin{aligned}
|\langle e|\sin\phi|g\rangle| &\simeq \frac{1}{2} |\langle \uparrow|\sin\phi|\uparrow\rangle - \langle \downarrow|\sin\phi|\downarrow\rangle| \\
&\simeq 1 - \frac{\tilde{J}}{N\hbar\tilde{\omega}_0}. \quad (\text{B2})
\end{aligned}$$

The terms $\langle \downarrow|\sin\phi|\uparrow\rangle$ are of order $\exp[-\tilde{\mathcal{S}}/\hbar]$ and hence negligible in the weak tunneling regime. Similarly, we also find

$$|\langle e|\sin^3\phi|g\rangle| \simeq 1 - 3\frac{\tilde{J}}{N\hbar\tilde{\omega}_0}. \quad (\text{B3})$$

APPENDIX C: EFFECTIVE LAGRANGEAN FOR AN OPEN AF SPIN CHAIN

In this appendix we show that an open spin chain with an odd number $N - 1$ of spins \mathbf{s}_i , $i = 2, 3, \dots, N$, can be mapped onto the Lagrangean of a modified FW. For simplicity we restrict ourselves to the chain

$$H = J \sum_{i=2}^{N-1} \hat{\mathbf{s}}_i \cdot \hat{\mathbf{s}}_{i+1} + \hbar\mathbf{h} \cdot \sum_{i=2}^N \hat{\mathbf{s}}_i - k_z \sum_{i=2}^N \hat{s}_{i,z}^2. \quad (\text{C1})$$

Again, we assume that the system exhibits AF order, and use the staggering $\mathbf{s}_i = (-1)^i s\mathbf{n} + \mathbf{l}$ for the spin fields, with $\mathbf{l} \cdot \mathbf{n} = 0$. Spatial variations of the fields \mathbf{n} and \mathbf{l} are strongly suppressed in the small system under consideration. We hence can proceed as in Sec. IV and carry out the Gaussian integral over \mathbf{l} . We obtain

$$\begin{aligned}
L_{\text{chain}}[\mathbf{n}] &= \frac{(N-1)^2}{8J(N-2)} [-(\mathbf{h} + h_A n_z \mathbf{e}_z - i\mathbf{n} \times \dot{\mathbf{n}})^2 \\
& + ((\mathbf{h} + h_A n_z \mathbf{e}_z) \cdot \mathbf{n})^2] - (N-1)k_z s^2 n_z^2 \\
& - s(\mathbf{h} \cdot \mathbf{n} - i\dot{\phi}(1 + \cos\theta)), \quad (\text{C2})
\end{aligned}$$

where $h_A = -2sk_z/(N-1)\hbar$. Evidently, by appropriate definition of \tilde{J} and $\tilde{\omega}_0$, the Lagrangean of the open spin chain can be mapped onto that of the modified FW [Eq. (31)] with excess spin $\delta s = s$.

-
- ¹ I. Ya. Korenblit and E. F. Shender, Sov. Phys. JETP **48**, 937 (1978).
 - ² E. M. Chudnovsky and L. Gunther, Phys. Rev. Lett. **60**, 661 (1988).
 - ³ *Quantum tunneling of magnetization*, L. Gunther and B. Barbara (eds.) (Kluwer, Dordrecht, 1994).
 - ⁴ J. R. Friedman, M. P. Sarachik, J. Tejada, and R. Ziolo, Phys. Rev. Lett. **76**, 3830 (1996).
 - ⁵ L. Thomas, F. Lioni, R. Ballou, D. Gatteschi, R. Sessoli, and B. Barbara, Nature **383**, 145 (1996).
 - ⁶ W. Wernsdorfer and R. Sessoli, Science **284**, 133 (1999).
 - ⁷ B. Barbara and E. M. Chudnovsky, Phys. Lett. A **145**, 205 (1990).
 - ⁸ I. V. Krive and O. B. Zaslavski, J. Phys. Cond. Matt. **2**, 9457 (1990).
 - ⁹ D. Gatteschi, A. Caneschi, L. Pardi, and R. Sessoli, Science **265**, 1054 (1994).
 - ¹⁰ K. L. Taft, C. D. Delfs, G. C. Papaefthymiou, S. Foner, D. Gatteschi, and S. J. Lippard, J. Am. Chem. Soc. **116**, 823 (1994).
 - ¹¹ A. Caneschi, A. Cornia, A. C. Fabretti, S. Foner, D. Gatteschi, R. Grandi, and L. Schenetti, Chem. Eur. J. **2**, 1379 (1996).
 - ¹² O. Waldmann, J. Schülein, R. Koch, P. Müller, I. Bernt, R. W. Saalfrank, H. P. Andres, H. U. Güdel, and P. Alenspach, Inorg. Chem. **38**, 5879 (1999).
 - ¹³ O. Waldmann, R. Koch, S. Schromm, J. Schülein, P. Müller, I. Bernt, R. W. Saalfrank, and F. Hampel, Inorg. Chem. **40**, 2986 (2001).
 - ¹⁴ A. Chiolerio and D. Loss, Phys. Rev. Lett. **80**, 169 (1998).
 - ¹⁵ B. Normand, X. Wang, X. Zotos, and D. Loss, Phys. Rev. B **63**, 184409 (2001).
 - ¹⁶ A. Cornia, A. Fort, M. G. Pini, and A. Rettori, Europhys. Lett. **50**, 88 (2000).
 - ¹⁷ J. N. S. Evans, *Biomolecular NMR Spectroscopy* (Oxford University Press, Oxford, 1995).

- ¹⁸ D. D. Awschalom, J. F. Smyth, G. Grinstein, D. P. DiVincenzo, and D. Loss, Phys. Rev. Lett. **68**, 3092 (1992).
- ¹⁹ D. D. Awschalom, D. P. DiVincenzo, and J. F. Smyth, Science **258**, 414 (1992).
- ²⁰ S. Gider, D. D. Awschalom, T. Douglas, S. Mann, and M. Chaparala, Science **268**, 77 (1995).
- ²¹ D. Loss, D. P. DiVincenzo, and G. Grinstein, Phys. Rev. Lett. **69**, 3232 (1992).
- ²² J.-M. Duan and A. Garg, J. Phys. Cond. Matt. **7**, 2171 (1995).
- ²³ E. M. Chudnovsky, J. Mag. Mag. Mat. **140-144**, 1821 (1995).
- ²⁴ A. Chiolero and D. Loss, Phys. Rev. B **56**, 738 (1997).
- ²⁵ B. A. Ivanov and V. E. Kireev, JETP Lett. **69**, 398 (1999).
- ²⁶ D. Awschalom, private communication; A. Cornia, private communication.
- ²⁷ F. Meier and D. Loss, Phys. Rev. Lett. **86**, 5373 (2001).
- ²⁸ R. Lü, P. Zhang, J.-L. Zhu, and L. Chang, Phys. Rev. B **56**, 10993 (1997).
- ²⁹ R. Lü, H. Hu, J.-L. Zhu, X.-B. Wang, L. Chang, and B.-L. Gu, Eur. Phys. J. B **14**, 349 (2000).
- ³⁰ Classical spin vectors are denoted without hat.
- ³¹ A. Cornia, A. G. M. Jansen, and M. Affronte, Phys. Rev. B **60**, 12177 (1999).
- ³² In order to obtain reliable results for the magnetization $M_x(B_x)$ with instanton techniques, one needs anisotropies as large as $k_z = 0.015J$ ($k_z = 0.039J$) in Fe_{10} (Fe_6) wheels. These values are larger than, but of the same order of magnitude as the ones of the clusters synthesized so far.
- ³³ Terms $\mathcal{O}((\omega_0/h_x)^2)$ can be neglected.
- ³⁴ H. Kleinert, *Path Integrals in quantum mechanics, statistics, and polymer physics* (World Scientific, Singapore, 1995).
- ³⁵ $M_\alpha = 0$ for $\alpha = y, z$ holds as long as $h_\alpha = 0$, independent of the magnitude of h_x .
- ³⁶ A. Auerbach, *Interacting Electrons and Quantum Magnetism* (Springer, New York, 1994).
- ³⁷ H.-B. Braun and D. Loss, Int. J. Mod. Phys. B **10**, 219 (1996).
- ³⁸ D. Loss in *Dynamical Properties of Unconventional Magnetic Systems*, A.T. Skjeltrop and D. Sherrington (eds.) (Kluwer, Dodrecht, 1998).
- ³⁹ M. Affronte, J. C. Lasjaunias, A. Cornia, and A. Caneschi, Phys. Rev. B **60**, 1161 (1999).
- ⁴⁰ The absolute value of $\delta B_{c,n}$ deviates from $4\tilde{J}/Ng\mu_B$ by terms of order $\tilde{\omega}_0^2/h_x^2$, which is beyond the precision of our result Eq. (35). Hence we compare ED and analytical results only for $\delta B_{c,n}(J') - \delta B_{c,n}(J)$, for which this shift nearly cancels.
- ⁴¹ Note that the classical value for m_z at the saddle points of the path integral, $\phi = \pi/2$ and $3\pi/2$, respectively, coincides with the value derived from the classical vector model in Sec. III, as it should.
- ⁴² S. Allen and D. Loss, Physica A **239**, 47 (1997).
- ⁴³ Terms proportional to $\cos\phi$ in m_z lead only to small contributions of order $\exp[-\tilde{S}/\hbar]$ to $|\langle e|\hat{m}_z|g\rangle|$. This allows us to neglect the term $i\dot{\theta}_0 \cos\phi$ [Eq. (42)].
- ⁴⁴ However, we do *not* claim that this is an indication that our ansatz Eq. (26) provides a full *microscopic* description of the local spin directions.
- ⁴⁵ Note that also the anisotropy energy favors a spin configuration as sketched in Fig. 3c such that the condition $h_x \gg |\delta s|8J/N$ can be relaxed. Consequently, also for Ga dopants a tunneling scenario is feasible.
- ⁴⁶ J. G. E. Harris, J. E. Grimaldi, D. D. Awschalom, A. Chiolero, and D. Loss, Phys. Rev. B **60**, 3453 (1999).
- ⁴⁷ A. Garg, Europhys. Lett. **22**, 205 (1993).
- ⁴⁸ V. Yu. Golychev and A. F. Popkov, Europhys. Lett. **29**, 327 (1995).
- ⁴⁹ J. Schnack and M. Luban, Phys. Rev. B **63**, 014418 (2001).
- ⁵⁰ A. Cornia, private communication.
- ⁵¹ A. Lascialfari, private communication.
- ⁵² E. M. Chudnovsky and D. A. Garanin, cond-mat/0105195.
- ⁵³ K. Park, M. A. Nowotny, N. S. Dalal, S. Hill, and P. A. Rikvold, cond-mat/0106276.
- ⁵⁴ K. M. Mertes, Y. Suzuki, M. P. Sarachik, Y. Paltiel, H. Shtrikman, E. Zeldov, E. Rumberger, D. N. Hendrikson, and G. Christou, cond-mat/0106579.